SOME INVESTIGATIONS ON ELECTROMAGNETIC WAVE PROPAGATION THROUGH SIMULATED PLASMA IN K-BAND

A Thesis
Submitted in Partial Fulfilment of the
Requirements for the Degree of
MASTER OF ENGINEERING
in Electrical Communication Engineering

By

D. V. GIRI

Department of Electrical Communication Engineering
Indian Institute of Science
Bangalore-12
1969

Contents

List of Symbols

d	:	Spacing between the wires
a	:	Spacing between 2 structures
λ_o	:	Free space wavelength (1.25 cm)
ω_p	:	Angular plasma resonant frequency
n	:	Refractive index
N	:	Plasma density
μ_r	:	Relative permeability
ϵ_r	:	Relative permittivity
μ_o	:	Free space permeability
ϵ_o	:	Free space permittivity
m	:	Mass of the electron
e	:	Charge of the electron
l	:	Plasma thickness
p	:	Broadside of the horn aperture

List of Illustrations

Photograph No

1	:	2K.33 Klystron power supply
2	:	Microwave components
3	:	Slow motion drive to vary the distance of separation between plasma structures
4, 5, 6	:	Plasma structures
7	:	Experimental set-up

TITLE

'Some investigations on electromagnetic wave propagation through simulated plasma in K band'

OBJECT

The object of the project work is to carry out investigations on the propagation characteristics of electro-magnetic waves in the K band when an artificial dielectric having effective dielectric constant less than unity is excited by radiation from a suitable source. In the present study, the plasma is simulated by a wire grid structure. The problem includes the following investigations:

(i) Variation of the effective dielectric constant as a function of the spacing of the wires '(d)' in the grid structure and the spacing'(a)' between two such structures,

(ii) Simulated plasma frequency as a function of 'a',

(iii) Propagation constant of the wave through the plasma as a function of 'a' and 'd',

(iv) Attenuation and phase constants of the wave passing through the simulated plasma.

The problem also includes the study of the shift in the peak of the major lobe of the radiation from a pyramidal horn when it passes through the plasma and the change in the character of the beam emerging from the plasma.

SUMMARY OF THE WORK

I. CONSTRUCTIONAL

a. Electronic Equipments

i. A high voltage regulated power supply unit for feeding a K Band 2K 33 Reflex Klystron,

ii. A square wave generator unit for modulating the reflector voltage of 2K 33 Klystron.

The above mentioned equipments have been constructed jointly with Sqn. Ldr. Lakhmir Singh.

b. Microwave components

i. Microwave components namely K-Band pyramidal horns, 1 crystal detecting section and waveguide adapter for matching 2K 33 klystron output to the transmitting horn have been designed and fabricated,

ii. Single and crossed wire grid structures using 36-SWG copper wires have been constructed to simulate lossless, homogeneous plasma,

iii. Single wire grid structures using 36-SWG Nichrome wire have been constructed to simulate lossy, homogeneous plasma.

II. THEORETICAL

i. Calculation of the radiation diagram of the pyramidal horn without plasma.

ii. Calculation of the radiation diagram of the pyramidal horn with plasma.

iii) Calculations of plasma frequency, ion density, effective dielectric constant, refractive index, propagation constant, attenuation and phase constants have been made from the physical parameters of the grid structure.

b) EXPERIMENTAL

i. Measurement and verification of the theoretical pattern of the pyramidal horn without plasma.

ii. Measurement of the radiation pattern of the horn with plasma.

The radiation diagrams have been studied as a function of the spacing between 2 plasma sheets.

><><><

Chapter I.

INTRODUCTION

The study of electromagnetic wave propagation through various types of media such as air, Ionosphere, Troposphere etc., has been a subject of considerable importance with reference to transmission of messages and signals from one terminal to the other. Modern communication requires the use of Microwave frequencies for sending messages from one point to another. The study of propagation characteristics of microwaves through plasma has assumed special significance with the advent of Space communication. Several problems in this context namely the Blackout of signals during the reentry of Space vehicles, loss of signal when it passes through the atmosphere containing Rocket exhaust, have been noticed in connection with the launching and reentry of Space vehicles. It has been suggested in Literature that the failure of the signals between the Space vehicle and the earth during the reentry period is probably due to trapping or total reflection of the electromagnetic wave by the plasma layer formed due to the thermal ionization arising due to the high aerodynamic drag between the earth's atmosphere and the Space vehicle which causes a temperature rise in the surroundings of the space vehicle, sometimes possibly of the order of $6000^{\circ}K$. The trapping of the wave may be due to the fact that the plasma formed round the space vehicle is of such thickness and ion density that the Sheath forms a surface wave structure. The formation of a surface wave structure may lead to trapping of the wave due to the nature of the surface wave phenomenon. The trapping of the em wave may also be due to the formation of a Duct inside the plasma layer

due to the gradient of ion density. The total reflection of the wave may be due to the fact that Brewster's angle which is related to the dielectric constant may be appropriate to prevent transmission through the plasma layer. This is frequency dependent due to the dispersive nature of the plasma medium. In order that the communication through the plasma layer may be uninterrupted, it is necessary to study the transmission coefficient or in other words the transmission ability of the plasma layer as a function of the ion density of the plasma, the frequency and angle of incidence of the incident wave. The study can be undertaken conveniently inside the laboratory with the help of an actual plasma created within a bounded medium by a discharge through gases, where the density of the plasma can be controlled by varying the pressure of the gas. However the study of plasma characteristics in this way, leads to several experimental difficulties such as (i) the creation of a homogeneous plasma, (ii) a stable plasma, and (iii) a large dimension plasma tube to avoid diffraction effects of the incident wave.

In view of the above mentioned difficulties regarding the homogeneity, the stability of plasma and the diffraction effects by the walls of the plasma container, it has been thought worthwhile to simulate the plasma by means of an artificial dielectric whose dielectric constant is less than unity. There are such artificial dielectrics at microwave frequencies namely, parallel plate dielectrics[1], wire grid structures[2] etc. whose properties of transmission, reflection at microwave frequencies have

been theoretically and experimentally studied extensively by Carlson Heins[3], Chatterjee et-all[4], Wait[5], Brown[6], Macfarlane[7], Ignatousky[8].

In the present investigation the plasma has been simulated artificially by means of wire grid structures for the following reasons.

i) construction is comparitively easier than parallel plate dielectrics,

ii) the lossy plasma can be simulated easily by using resistive wires instead of copper wires,

iii) crossed wire type structure can easily be constructed. It is difficult to adopt this type of structure in the case of parallel plate dielectrics.

Crossed wire type of structure provides an opportunity of studying the character of the emergent beam when only a Vertically or Horizontally polarized wave is incident on the structure. It is believed at first sight that the horizontal wires of the crossed structure should not have any significant influence when the incident wave is vertically polarized and vice-versa, but the experimental results show that the horizontal wires do have appreciable influence on the character of the emergent beam, even when the incident wave is only vertically polarized. This has not been explained by rigorous mathematical reasoning.

In the experimental investigations, the radiation patterns of a pyramidal horn with and without plasma have been studied. The result shows that the peak of the major lobe of the Horn without any intervening plasma occurs as expected along the axis. But a significant shift in the position of the major lobe occurs due to the intervening plasma. It has also been observed experimentally that the radiation pattern of the horn is modified considerably due to the presence of plasma. Cases have been observed where there is a single sharp peak with a few minor lobes. In other cases, depending on the distance between the plasma sheets, the major lobe has been split up into two almost equal lobes. In certain other cases, the major lobe is split up into two lobes whose amplitudes are different. Several reasons for this kind of a behaviour have been given qualitatively in the section on discussion. The shift of the majorlobe yields a method of calculating the plasma density of an actual plasma which will give the same amount of shift. It has not been possible to use the distortion in the radiation diagram for finding out what equivalent characteristics this has in relation to an actual plasma.

There is one drawback however in the study of simulated plasma with an attempt to correlate its characteristics to an actual plasma, in that the effect of the magnetic field on the propagation characteristics of electromagnetic waves through simulated plasma is not possible at the present stage of laboratory technique. It is due to this technical drawback that the

study of such interesting electromagnetic phenomenon like the splitting of the wave into ordinary and extraordinary rays, Faraday rotation, has not yet been possible with the help of simulated plasma. However, it is hoped that the results of the present investigations will add to a certain extent to some aspects of our existing knowledge of the propagation characteristics of electromagnetic waves through plasma. It is also hoped that this type of investigation will lay the foundation for a study of plasma diagnostics in the laboratory with the help of artificial plasmas. It is believed that this is a very fruitful line of investigation about which very little is reported in the literature either on the theoretical or the experimental areas. This investigation is to be regarded as only a starting point for further intense work with different types of structures which would simulate a natural plasma.

-oOo-

Chapter II.

THEORETICAL

1. RADIATION PATTERN OF THE PYRAMIDAL HORN IN FREE SPACE

An identical pair of horns is designed to give a single sharp lobe in H-plane. The power pattern is given by the following relation.

$$P_\phi \quad \propto^{l} \left[\frac{\frac{\pi^2}{4}\cos\theta \quad \cos\left(\frac{K_o p}{2}\sin\theta\right)}{\left(\frac{\pi}{2}\right)^2 - \left(\frac{K_o p}{2}\right)\sin^2\theta} \right]^2 .$$

'K_o' = free space wave no.

'p' = Broadside of the horn aperture

The above equation is derived on the basis of aperture current distribution considerations. It has been assumed that the distribution is not affected by the edges of the pyramidal horn. Using the above relation, the free space H plane radiated power pattern has been calculated and plotted. (Fig. 6)

2. RADIATION PATTERN OF THE PYRAMIDAL HORN WITH PLASMA

Richmond and Neugebauer[10] have shown that the Radiation diagram of an antenna behind a dielectric obstacle can be described as the free space radiation pattern of the antenna modified by the plane wave transmission coefficient for the dielectric obstacle. Thus

$$\bar{E}(\theta) = T(\theta)\ \bar{E}_o(\theta)$$

$\bar{E}(\theta)$ = far field electric vector of the source in the presence of the dielectric obstacle

$\bar{E}_o(\theta)$ = far field electric vector of the source in the absence of the dielectric obstacle

$T(\theta)$ = plane wave transmission coefficient of the dielectric obstacle.

For a plasma slab model, the transmission coefficient for normal incidence has been derived and the power pattern is given by

$$P_\phi \propto \left[\frac{\pi^2}{4}\cos\theta \frac{\cos\left(\frac{K_o p}{2}\sin\theta\right)}{\left(\frac{\pi}{2}\right)^2 - \left(\frac{K_o p}{2}\right)\sin^2\theta}\right]\left[\frac{1}{\cos^2(K_z l) + \left(\frac{\cos^2\theta}{n^2-\sin^2\theta}\right)\sin^2 K_z l}\right]$$

K_z = Z component of wave no. = $K_o\sqrt{n^2-\sin^2\theta}$

n = refractive index of plasma

l = distance of travel in plasma or plasma thickness.

Chapter III.

EXPERIMENTAL

In order to carry out the experimental investigations on the characteristics of the simulated plasma, some electronic equipments and microwave components as well as the plasma structures as follows have been constructed.

I. ELECTRONIC EQUIPMENTS

A high voltage regulated power supply is constructed to operate 2K 33, (RAYTHEON) K Band Reflex Klystron Oscillator. This d.c. power source consists of separately regulated Beam, Reflector and Focus grid Voltage supplies. The equipment also provides an unregulated a.c. heater voltage for the klystron. All the controls required to operate the power supply are on the front panel. Separate meters on the front panel read Beam voltage, Beam current, reflector voltage and grid voltage. The complete power supply is housed in a rugged frame approximately 48" high x 20" wide x 16" deep. The circuit diagram has been shown in fig. 1. The power supply uses the conventional procedure of using a step up transformer at line frequency, then rectifying and regulating the transformer output voltage.

OPERATING PRINCIPLE:

The high voltage from the step up transformer is given to a full wave rectifier consisting of a pair of H.V. rectifiers (866 A). The rectified voltage is passed through an L.C. π section filter network before it feeds an electronic regulator

unit. The control of the output voltage of the main supply is accomplished by the tubes 6 SH7 and 807. The voltage which appears at the grid of 6 SH7 is the difference between a voltage taken from a divider across the output voltage and a fixed bias voltage provided by a regulator reference tube. The constant bias provided by the regulator reference tube, in particular the independence of this bias on the plate current of regulator amplifier 6SH7, is essential for the operation of the system. The control grid of the Regulator tube 807 is activated by the regulator amplifier and the adjustment of the bias for the regulator amplifier by means of a variable resistor provides the means of controlling the output voltage of the power supply within the limits of 1200 to 2300 volts. Another variable resistor adjusts the feed back to the control tube and must be set for the amount of feedback giving the best regulation. To supply the reflector voltage, there is a separate rectifier 5R4GY the output of which passes through a π section filter before it activates five VR tubes connected in series. The regulated reflector voltage is obtained by tapping off from a voltage divider placed across the VR tubes. The -Ve focus grid voltage is obtained from a variable resistor connected across a VR tube which is immediately in series with the regulator reference VR tube.

For the sake of operational safety, the Beam electrode of the klystron is held at ground potential and the cathode is fed with a high negative potential.

OUTPUT VOLTAGE RANGES WITH RESPECT TO CATHODE

a. BEAM VOLTAGE

i) voltage range : 1200 to 2300 v. electronically regulated

ii) Regulation : ± 0.5 volts d.c. max at a setting of 1800 v at 10 ma for ± 10 % input voltage variation.

b. REFLECTOR VOLTAGE

i) Voltage Range: 0 to − 750 v. with coarse and fine controls.

c. FOCUS GRID VOLTAGE

i) Positive 0 to + 150 v. Regulated

ii) Negative 0 to − 150 v. Regulated

d. HEATER VOLTAGE

6.3 volts a.c. unregulated, with a provision for control to account for large input line voltage fluctuations.

I (b) A square wave generator unit for modulating the reflector of the klystron has also been constructed. The circuit diagram has been shown in fig. 1.

The square wave generator has its own VR tube regulated voltage supply. The square wave is provided by a multivibrator, amplifier and square wave shaper and clipper. The resultant square wave has rise and fall times of about 1 μs. The frequency of the output may be varied from 350 to 3500 Hz.

The amplitude of the square wave may be varied from 0 to 100V. The square wave voltage is capacitance coupled to the reflector with provision for switching to an external source of modulation if desired. A diode clipper tube 6 x 5, is used from cathode to the reflector to prevent the reflector from becoming + ve w.r.t. cathode.

II. MICROWAVE COMPONENTS

(a) Pyramidal Horns:

An identical pair of optimum pyramidal horns were designed and fabricated. The dimensions of the pyramidal horn and other constructional details are shown in the fig.2. Theoretically this pyramidal horn is meant to give a single sharp lobe in the H plane. The designed half power beam width for the horn is 12^{o}.

(b) A detecting section incorporating an IN26 crystal has also been fabricated. (Photograph 2)

(c) A slow motion drive to vary the separation between 2 sheets is fabricated. Provision is made to vary the separation distance from 0 to 4 cms. (Photograph 3)

III. PLASMA STRUCTURES

The plasma structures which have been constructed are shown in photographs 4, 5 and 6.

CONSTRUCTION: Square frames of inner dimension of 20 cms x 20 cms are first cut from 1/16" thick PVC sheets. Copper cladded Bakelite sheets are fixed to the PVC frames on one side with the help of Araldite. By a process of acid etching copper is retained in the form of strips of suitable dimensions on opposite sides of the frame for a single wire type of structure. Holes of a suitable diameter are drilled on these copper strips. 36 SWG copper wire (without enamel) is stretched in these holes and is soldered at either ends taking care to see that the wire is sufficiently taut and straight. The holes into which the wires are soldered are drilled at regular intervals so that the spacing between the wires is maintained uniform throughout. The spacing between the wires and the diameter of the wire have to be small compared to wavelength. Practical limitations decide the spacing and wire diameter to be 4 mms and 0.192 mm. respectively. The structure has an over-all dimension of 20 cms x 20 cms. This is approximately 15 times wavelength square and is expected to avoid all the diffraction effects.

The cross wire type of structure is also constructed in a similar manner with spacing of 4 mm in either direction. A few structures with resistive wires to simulate a lossy plasma, have also been constructed.

The Radiation diagram of the Horn was obtained by the usual method of keeping the transmitter horn fixed in one arm of the Spectrometer Table and rotating the receiving horn mounted on the other arm. The experimental set up is shown in photograph 7. The Radiation diagram of the Horn without plasma has been plotted (Fig. 7). The theoretical pattern is drawn with full line and the experimental pattern is shown by dotted circles.

The single wire type structures are mounted on a platform provided with a slow motion drive to vary the separation. A large number of radiation diagrams were obtained for different distances of separation between the two sheets. The results are plotted in fig. 7 - 9.

The crossed wire type of plasma sheets were then introduced between the transmitter and the Receiver Horns and the radiation diagrams were obtained for various distances of separation between the two sheets. The results are plotted in fig.9 - fig. 11. The results with lossy structures are plotted in fig. 12 - fig. 14.

NUMERICAL CALCULATIONS

Several parameters of interest such as dielectric constant, refractive index, plasma frequency, propagation constant, attenuation and phase constants, plasma density have been calculated from the physical parameters of the plasma structure. The results are reported in a tabular form in Table 1.

Description → Physical parameters in mms.	a = 3mm d = 4mm ρ = .096 mm λ = 12.5mm	a = 4 d = 4 ρ = .96 λ = 12.5	a = 5 d = 4 ρ = .96 λ = 12.5	a = 6 d = 4 ρ =.096 λ = 12.5	a = 9 d = 4 ρ = .096 λ = 12.5	a = 10 d = 4 ρ = .096 λ = 12.5	a = 11 d = 4 ρ = .096 λ = 12.5	a = 12 d = 4 ρ = .096 λ = 12.5
Dielectric constant ϵ_r	0.131	0.405	0.584	0.789	0.565	0.710	0.784	0.865
Plasma freq. f_p	22.8 GHz	18.5GHz	11.8GHz	11 GHz	15.6GHz	12.9 GHz	11.2 GHz	8.8 GHz
Polarization of the incident wave	Horizontal	Horizon-tal	Hori-zontal	Horizon-tal	Horizon-tal	Horizontal	Horizontal	Horizontal
Nature of incidence	Normal	Normal	Normal	Normal	Normal	Normal	Normal	Normal
Propagation constant $\gamma = \alpha + j\beta$	j.182 rad/cm	j.06 rad/cm	j.70 rad/cm	j.1.31 rad/cm	j.64 rad/cm	j1.09 rad/cm	j1.31 rad/cm	j1.53 rad/cm
No density of plasma N	$6.45 \times 10^{18}/m^3$	$4.25 \times 10^{18}/m^3$	$1.74 \times 10^{18}/m^3$	$1.5 \times 10^{18}/m^3$	$3.15 \times 10^{18}/m^3$	$2.06 \times 10^{18}/m^3$	$1.53 \times 10^{18}/m^3$	$.955 \times 10^{18}/m^3$

TABLE - I.

Some sample calculations are shown below:

1) Dielectric constant = ϵ_r = (refractive index n)^2.

'n' is calculated from

$$\cos\left(\frac{2\pi a n}{\lambda}\right) = \left\{ \cos\left(\frac{2\pi a}{\lambda}\right) + \frac{\lambda}{2d} \frac{\sin\left(2\pi a/\lambda\right)}{\log_e\left(\frac{d}{2\pi\rho}\right) + F\left(d/\lambda\right)} \right\}$$

ex: a = 5 mm
d = 4 mm
ρ = 0.096 mm
λ = 12.5 mm

$F(d/\lambda)$ = correction term available in Tables.

$F(4/12.5)$ = 0.07

$$\cos\left(\frac{2\pi a n}{\lambda}\right) = \cos 144^\circ + \frac{12.5}{8} \frac{\sin 144^\circ}{\log_e\left(\frac{4}{2 \times 3.14 \times .096}\right) + .07}$$

$\cos(144n)^\circ = -\sin 54^\circ + .795 \cos 54^\circ$

$\cos(144n) = -0.809 + .468$

or $\cos(144\ n) = -.343$

$\therefore$ Refractive index n = .764

Dielectric constant ϵ_r = 0.584

2) Calculation of plasma frequency

Ex: 1. $a = 4$ mm

$d = 4$ mm

$\rho = 0.096$ mm

$f = 24$ GHz or $\lambda = 12.5$ mm

$$\epsilon_r = 0.405 = n^2$$

$$f_p = f\sqrt{1 - n^2}$$

$$= 24\sqrt{1 - 0.405} = 24\sqrt{.595}$$

$$= 24 \times 0.772$$

$$f_p = 18.5 \text{ GHz}$$

EX: 2. $a = 9$ mm

$d = 4$ mm

$\rho = 0.096$ mm

$\lambda = 12.5$ mm or $f = 24$ GHz

$\epsilon_r = 0.565$

$$f_p = f\sqrt{1 - n^2}$$

$$= 24\sqrt{1 - .565} = 24\sqrt{.435}$$

$$= 24 \times .658$$

$$f_p = 15.7 \text{ GHz}$$

---

3. Calculation of propagation constant

$$\gamma^2 = -\omega^2 \mu \epsilon$$

$$= -\omega^2 \mu \epsilon_o \left(1 - \frac{f_p^2}{f^2} \right)$$

$$= -\frac{\omega^2}{c^2} \left(1 - \frac{f_p^2}{f^2} \right)$$

$$= -\frac{\omega^2}{c^2} \epsilon_r$$

or $$\gamma = +j \frac{\omega}{c} \sqrt{\epsilon_r}$$

$$= j\ 5.04 \sqrt{\epsilon_r}\ \text{rad/cm}$$

ex 1.

$a = 3$ mm

$d = 4$ mm

$\rho = 0.096$ mm

$\lambda = 12.5$ mm

$\epsilon_r = 0.131$

$$\gamma = j\ 5.04 \times \sqrt{.131}\ \text{rad/cm.}$$

$$\gamma = j\ 1.82\ \text{rad/cm}$$

ex 2.

$a = 5$ mm

$d = 4$ mm

$\rho = 0.096$ mm

$\lambda = 12.5$ mm.

$\epsilon_r = 0.584$

$$\gamma = j\,5.04 \times \sqrt{.584} = j\,3.84 \text{ rad / cm}$$

$$\gamma = j\,0.70 \text{ rad / cm}$$

4. Calculation of plasma density

from $\omega_p^2 = \frac{Ne^2}{m\,\epsilon_o}$ we find

$$N = 1.24^2 \times 10^{-2} \times f_p^2 \text{ / } M^3.$$

ex.1. $a = 5$ mm

$d = 4$ mm

$\rho = 0.096$ mm

$\lambda = 12.5$ mm

$\epsilon_r = 0.584$

$f_p = 11.8$ GHz

$\therefore \quad N = 1.242 \times 10^{-2} \times (11.8)^2 \times 10^{18/M^3}$

$$N = 1.74 \times 10^{18} \text{ / } M^3$$

ex. 2

$a = 4$ mm

$d = 4$ mm

$p = 0.096$ mm

$\lambda = 12.5$ mm

$\epsilon_r = 0.405$

$f_p = 18.5$ GHz

$$N = 1.242 \times 10^{-2} \times (18.5)^2 \times 10^{18} / M^3$$

$$N = 4.25 \times 10^{18/M^3}$$

Calculation of

H plane Radiation diagram of the Horn without plasma. TABLE II.

$$P_\phi \quad \alpha' \quad \left\{ \frac{\pi^2}{4} \cos\theta \; \frac{\cos\left(\frac{\pi p}{2} \sin\theta\right)}{\left(\frac{\pi}{2}\right)^2 - \left(\frac{\pi p}{\lambda}\right) \sin^2\theta} \right\}^2$$

p = Broad side of the Horn Aperture = 7.62 cms.

θ Deg.	cos θ	sin θ	$\frac{\pi p \sin\theta}{\lambda}$	$\cos\left(\frac{\pi p \sin\theta}{\lambda}\right)$	$\left(\frac{\pi p \sin\theta}{\lambda}\right)^2$	$\left(\frac{\pi p \sin\theta}{\lambda}\right)^2 - \frac{\pi^2}{4}$	E_ϕ	P_ϕ	Normalized P_ϕ
0	1.0	0	0	1.0	0	-2.464	-1	1	100
2	.9994	.0349	.6679	.785	.4461	-2.018	.958	.910	91
4	.9976	.0698	1.335	0.233	1.782	-.682	.842	.709	70.9
6	.9945	.1045	2.001	.416	4	1.536	.675	.455	45.5
8	.9903	.1392	2.664	.888	7.099	4.635	.470	.221	22.1
10	.9848	.1736	3.324	.983	11.05	8.586	.279	.0778	7.78
12	.9781	.2079	3.981	.666	15.85	13.386	.1205	.0145	1.45
14	.9703	.2419	4.63	.580	21.44	18.976	.101	.0102	1.02
16	.9613	.2756	5.277	.537	27.85	25.386	.05	.0025	.25

TABLE II. - CALCULATED H-PLANE RADIATION DIAGRAM OF THE HORN IN FREE SPACE. PLOT IS SHOWN IN FIG. 7.

EXPERIMENTAL RESULTS

A large no of experiments were performed for radiation patterns of the horn as a function of 'a' and only a few typical results are presented below in tabular form.

H plane radiation pattern of the horn without plasma. plot is shown in Fig. 7.

TABLE - III

Clockwise				Anticlockwise			
θ in Deg	Normalized power	θ in Deg	Normalized power	θ in Deg	Normalized power	θ in Deg	Normalized power
0	100	13	32	0	100	13	19
1	100	14	26	1	99	14	13
2	99	15	22	2	92	15	11
3	98	16	17	3	76	16	8
4	95	17	14	4	66	17	6.5
5	86	18	10	5	59	18	5
6	78	19	7	6	52	19	4
7	72	20	5	7	46	20	3
8	64	21	4	8	42	21	0
9	56	22	2.5	9	37	22	0
10	48	23	2	10	32	23	0
11	41	24	0	11	29	24	0
12	36	25	0	12	23	25	0

H plane radiation patternof the horn in the presence of lossless homogeneous plasma. Physical parameters of Y plasma are as follows.

d = 4 mm; a = 6 mm; ρ = .096 mm; λ = 12.5 mm

Plot is shown in Fig. 8.

TABLE IV.

Clockwise				Anticlockwise			
θ in Deg.	Normalized power	θ in Deg.	Normalized power	θ in Deg.	Normalized power	θ in Deg.	Normalized power
0	28	16	0	0	28		
1	26	17	2	1	40	17	14
2	40	18	4	2	48	18	13
3	49	19	3	3	70	19	8
4	60	20	1	4	92	20	2
5	60	21	0	5	100	21	2
6	40	22	0	6	84	22	4
7	24	23	0	7	60	23	0
8	10	24	0	8	40	24	0
9	8	25	0	9	26	25	0
10	4	26	0	10	16	26	0
11	4	27	0	11	10	27	0
12	0	28	1	12	6	28	0
13	0	29	4	13	6	29	3
14	0	30	0	14	4	30	4
15	0			15	6	31	4
				16	11	32	0.5
						33	0

H plane radiation pattern of the horn in the presence of lossless homogeneous plasma. Physical parameters of the XY plasma are as follows

d = 4 mm; a = 5 mm; δ = .096 mm; λ = 12.5 mm;

plot is shown in Fig. 10.

TABLE - V

Clockwise				Anticlockwise			
θ in Deg	Normalized	θ in Deg.	Normalized	θ in Deg.	Normalized power	θ in Deg	Normalized power
0	26	9	2	0	26	12	12
1	18	10	2	1	44	13	8
2	18	11	1	2	60	14	4
3	20	12	0	3	74	15	3
4	24	13	0	4	84	16	3
5	20	14	0	5	100	17	2
6	13			6	100	18	3
7	6			7	80	19	2
8	4			8	56	20	1
				9	36	21	0
				10	24	22	0
				11	16	23	0

H Plane radiation pattern of the horn in the presence of lossy, homogeneous plasma. Physical parameters of lossy Y plasma are as follows,

d = 4 mm; a = 10 mm, δ = .096 mm; λ = 12.5 mm ;

plot is shown in Fig. 14.

TABLE VI

Clockwise				Anticlockwise			
θ in Deg	Normalized power	θ in Deg	Normalized power	θ in Deg.	Normalized power	θ in Deg.	Normalized power
0	58	15	4	0	58	20	16
1	32	16	4	1	80	21	10
2	18	17	8	2	100	22	15
3	24	18	11	3	100	23	34
4	38	19	5	4	82	24	32
5	60	20	2	5	60	25	20
6	75	21	2	6	60	26	18
7	72	22	2	7	56	27	22
8	48	23	2	8	40	28	12
9	48	24	6	9	20	29	2
10	28	25	2	10	6	30	1
11	35	26	12	11	4	31	0
12	38	27	20	12	4	32	0
13	24	28	11	13	12	33	0
14	8	29	0	14	20	34	3
		30	4	15	10	35	6
		31	0	16	12	36	6
				17	22	37	4
				18	28	38	2
				19	18	39	0

Chapter IV
DISCUSSION

The experimental results show that the peak of the major lobe shifts when the plasma sheaths are introduced between the transmitter and receiver. Table VII shows the shift as a function of spacing in the three cases of lossless Y, lossless XY and lossy Y plasma. It will be observed that the shift as a function of 'a' differs in the three types of plasma. For ex: For a = 3 mms and 12 mms, the angle of shift in the case of lossless Y plasma is 6^{o} whereas in the case of lossless XY plasma, the same amount of shift occurs for spacing a = 4mms and 9 mms. It is believed that the shift is mainly due to the ion density of an actual plasma corresponding to the simulated plasma. If this is true, then it may be said that the plasma simulated by the XY structure for a = 4 and 9 mms will be the same as that represented by Y structure with a = 3 and 12 mms.

Table VIII gives the corresponding ion density calculated from the observed angular shift for lossless Y and XY plasma. The angle of shift, the ion density and the half power beam width of significant lobes have been tabulated and plotted.

TABLE-VII

Shift in the peak of the major lobe due to plasma, as a function of spacing 'a'.

Plot is shown in Fig. 3.

Spacing 'a' between two structures	Angle of shift		
	Lossless Y plasma	Lossless XY plasma	Lossy Y plasma
2 mms	-	4.5°	2°
3	6°	4.5°	2°
4	2°	6°	2°
5	5°	5°	0°
6	4.5°	3°	2°
7	-	4°	3°
8	-	5°	3°
9	4.5°	6°	3°
10	4.5°	6.5°	3°
11	7°	5°	2°
12	6°	5°	1°
13 mms	-	5.5°	0°

TABLE - VIII

Equivalent density calculated from the shift in the peak of the major lobe. Plot is shown in Fig. 4.

Lossless Y plasma

Spacing 'a' in mms	Shift in degree	Density /m^3
3	6	7.63×10^{16}
4	2	$.98 \times 10^{16}$
5	5	5.46×10^{16}
6	4.5	4.2×10^{16}
9	4.5	4.2×10^{16}
10	4.5	4.2×10^{16}
11	7	10.22×10^{16}
12	6	7.63×10^{16}

Lossless XY plasma

Spacing 'a' in mms	Shift in degrees	Density /m^3
2	4.5	4.2×10^{16}
3	4.5	4.2×10^{16}
4	6	7.63×10^{16}
5	5	5.46×10^{16}
6	3	1.96×10^{16}
7	4	3.57×10^{16}
8	5	5.46×10^{16}
9	6	7.63×10^{16}
10	6.5	8.96×10^{16}
11	5	5.46×10^{16}
12	5	5.46×10^{16}
13	5.5	6.44×10^{16}

Sample Calculation

$\cos(\text{Angle of shift}) = n = \sqrt{\epsilon_r} =$ Refractive index

$f_p = f\sqrt{1-n^2}$ = plasma frequency.

$N = 1.242 \times 10^{-2} \times f_p^2 / m^3$

Ex: Shift = 2^0

$n = \cos 2 = .9994$; $f = 24$ GHz

$f_p^2 = f^2(1-n^2) = (24)^2\ (.0014)\ (10^{18})$

$N = 1.242 \times 10^{-2} \times (24)^2 \times 10^{18} \times (.0014)$

$= .98 \times 10^{16} / m^3$

TABLE-IX Distortion of the Radiation Pattern in the case of lossless Y plasma. Half Power Beam widths are plotted in Fig. 5.

Spacing 'a' in mms	No.of lobes including the major lobe	Magnitude of each lobe	Position of each lobe w.r.t. axis	Half Power Beam widths
3	Two	1.00	6^{o} Anticlockwise	5^{o}
		.6	5^{o} Clockwise	8^{o}
4	Two	1.00	2^{o} Anticlockwise	6^{o}
		0.78	8^{o} Clockwise	6^{o}
5	Two	1.00	5^{o} Anticlockwise	5^{o}
		0.60	6^{o} Clockwise	5^{o}
6	Two	1.00	4.5^{o} Anticlockwise	6^{o}
		0.60	4^{o} Clockwise	4^{o}
9	Two	1.00	4.5^{o} Anticlockwise	5^{o}
		1.00	5^{o} Clockwise	4^{o}
10	One	1.00	4.5^{o} Anticlockwise	3.5^{o}
11	Two	1.00	7 Anticlockwise	5^{o}
		0.90	2 Clcokwsie	4^{o}
12	Two	1.00	6^{o} Anticlockwise	8^{o}
		0.80	3^{o} Clockwise	5^{o}

Table X: Distortion of the Radiation Pattern in the case of lossless XY plasma. Half power beam widths are plotted in Fig. 5.

Spacing 'a' in mms	No.of lobes including the major lobe	Magnitude of each lobe	Position of each lobe w.r.t.axis	Half Power Beam widths
2	one	1.00	6° Anticlockwise	8°
3	one	1.00	4.5° Anticlockwise	8°
4	one	1.00	4.5° Anticlockwise	10°
5	one	1.00	6° Anticlockwise	6°
6	Two	1.00 0.88	3° Anticlockwise 3° Clockwsie	8° 5°
7	Two	1.00 0.66	4° Anticlockwise 5° Clockwise	6° 4°
8	Three	1.00 0.84 0.80	5° Anticlockwise 1° Anticlockwise 4° Clockwise	4.5° 4° 4°
9	Two	1.00 0.84	6° Anticlockwise 4° Clockwise	4° 4°
10	Two	1.00 0.80	6.5° Anticlockwise 3° Clockwise	4° 3°
11	Two	1.00 0.58	5° Anticlockwise 4° Clockwise	6° 3°
12	One	1.00	5° Anticlockwise	6°
13	one	1.00	5.5° Anticlockwise	6°

TABLE XI Distortion of the Radiation pattern in the case of lossy Y plasma.

Spacing 'a' in mms	No.of lobes including the major lobe	Magnitude of each lobe	Position of each lobe w.r.t. axis	Half power Beam width
2	one	1.00	2° Anticlockwise	15°
3	one	1.00	2° Anticlockwise	14°
4	one	1.00	2° Anticlockwise	15°
5	one	1.00	Along the axis	12°
6	one	1.00	2° Clockwise	14°
7	two	1.00	3° Anticlockwise	11°
		0.58	8° Clockwise	8°
8	two	1.00	3° Anticlockwise	12°
		0.68	8° Clockwise	7°
9	two	1.00	3° Anticlockwise	6°
		0.92	6° Clockwise	4°
10	two	1.00	3° Anticlockwise	8°
		.76	6° Clockwise	5°
11	one	1.00	2° Anticlockwise	17°
12	one	1.00	1° Anticlockwise	12°
13	one	1.00	Along the axis	12°

Distortion in the Radiation Diagram

It is observed from the experimental results that the radiation patterns in the presence of plasma are distorted and the distortion depends on the spacing between two structures in all the three cases of lossless Y, lossless XY and lossy Y plasma. It will be further noticed that if we consider only comparitively larger lobes, it appears as if the main lobe of the horn without plasma is split into two portions. It is also seen that the half power beamwidths of significant lobes vary with 'a' and vary differently for the three types of plasma. For ex: Table XI shows that in the case of lossy Y plasma for a = 4 mms and d = 4 mms, the beam becomes very broad, the half power beamwidth being of the order of 15^{o}.

The changes in the radiation pattern including shift, beamwidth and distortion in the presence of plasma indicate the presence of either of the following two phenomenon.

1. The individual wires of the structure being excited by the incident wave acts as an independent source of radiation and the radiated field is consequently the resultant of the fields of the individual sources with due regard to amplitude and phase distributions. However for a rigorous calculation of the radiation diagram based on this approach, one should also consider the interaction between each element of the source.

2. The structure may be assumed to be an assembly of a large number of apertures with a proper field distribution and ignore the presence of the sources. This aperture field distribution is undoubtedly different from that of a pyramidal horn and hence the radiation diagrams with and without plasma differ.

The above discussion is purely qualitative but essentially outlines two well known mathematical approaches for calculation of radiation diagram of any type of antenna. In the former case, Green's function method is used where the presence of the source is taken into consideration and in the latter, only Huyghen sources simulate the field distribution and ignores the presence of the source.

Splitting of the Beam

Experiments show in certain cases that the main beam of the horn is split into 2 portions. We shall now attempt a qualitative explanation for the splitting of the beam.

From the Magneto ionic theory proposed by Appleton-Hartree , it is known that the splitting of the beam occurs into ordinary and extraordinary rays when an em wave is propagated through an ionized medium in the presence of a d.c. magnetic field and the extent of splitting depends on the strength of the magnetic field, its ordientation with respect to the direction of travel of the passing wave and the ion density of the medium. Appleton-Hartree relations give the refractive index of a plasma atmosphere as

$$n^2 = 1 + \frac{2}{2(\alpha+j\beta) - \frac{\gamma_T^2}{(1+\alpha+j\beta)} \pm \sqrt{\left\{\frac{\gamma_T^4}{(1+\alpha+j\beta)^2} + 4\gamma_L^2\right\}}}$$

where

n^2 = (refractive index)^2

α = $-\omega^2/\omega_p^2$.

ω = angular frequency of the wave,

ω_p = angular plasma resonant frequency,

ν = collisional frequency,

β = $\omega\nu/\omega_p^2$,

γ_L = $\omega\omega_L/\omega_p^2$,

γ_T = $\omega\omega_T/\omega_p^2$,

ω_L = $\frac{H_L e}{mc}$,

ω_T = $\frac{H_T e}{mc}$,

H_L = Component of magnetic field along the direction of propagation,

H_T = Component of magnetic field along the transverse direction.

It will be noticed from the Appleton-Hartree relation that for a particular value of the d.c. magnetic field, two values of dielectric constants are possible.

Since a study of the effects of a d.c. magnetic field is not directly possible with the simulation technique, we may consider that the wave incident on the wire grid induces electric currents in each of the wire, which generate local magnetic field. If we consider the incident wave to be plane, we may say that currents induced in each wire have the same phase relation and hence the local magnetic field will be additive. This justifies the presence of the magnetic field. We will now proceed to calculate the strength of this magnetic field through the Appleton-Hartree relation for a particular plasma slab.

Ex: Lossless Y Plasma

Calculated f_p = 8.8 GHz

Spacings in mms	No.of lobes observed	Relative magni-tudes	Position of the lobes w.r.t.axis	Dielectric constant
a = 12	Two	1.00	6^o Anticlockwise	0.089
d = 4		0.80	3^o Clockwise	0.996

TABLE XII: Distortion in the Radiation diagram

We shall now make certain approximations in the Appleton-Hartree relation and estimate the value of the magnetic field which gives rise to the two values of dielectric constants which have been experimentally observed for the structure described in Table XII. Assuming that there are no interparticle collissions (lossless plasma or $\nu = 0$) and that the d.c. magnetic field is entirely transverse ($H_L = 0$), we find that this magnetic field is of the order of 10^8 Amps/met. This explains the distortion of the radiation diagram partially and the splitting of the beam has been correlated to the extraordinary and the ordinary rays as given by Appleton-Hartree relations.

It is known that the magnetic field used in Appleton Hartree relation is a d.c. magnetic field where as in the present case, the magnetic field is time varying. In order to calculate a correct value of the magnetic field which will give the amount of splitting as observed experimentally, one needs to reformulate Appleton-Hartree relations with a time varying magnetic field. This subject is receiving further attention.

The simulated plasma experiments have been done inside the laboratory. It is therefore necessary to determine whether the experimental results are affected due to the environment. This is done by putting the plasma in different positions, maintaining the normal incidence of the beam. It has been found that the radiation pattern does not show any

noticeable change. Radiation diagrams have also been repeated in a few cases by altering the ffequency of the source slightly. In this case also no noticeable change in the diagram has been found. Hence it is concluded that the environment in which the experiment has been carried out does not have any significant effect on the results of the experiment. The experimental results may also be affected due to the diffraction of the wave from the edges of the plasma structure. To study the effect of diffraction, the position of the structure has been slightly altered from the centre of the spectrometer table sideways and vertically as well, no appreciable change is observed in the radiation diagram. This shows that the effect of diffraction from the edges of the structure is not significant.

It is believed that this attempt to set up a simulated plasma to study the behaviour of electromagnetic wave propagation, the calculation of the ionic density of an actual plasma and the calculation of the magnetic field to explain the splitting of the beam is a fruitful field of study. A much more exhaustive study on simulated plasma in the X, K and Q bands, is under progress. It is hoped that the results of these investigations will lead to a precise understanding of the behaviour of electromagnetic wave propagation through different types of plasma.

ACKNOWLEDGEMENT

The author expresses his thanks to Prof. S.V.C. Aiya for giving the encouragement and providing all the necessary facilities. The author is also grateful to Dr.(Mrs.) R. Chatterjee and Prof. S.K. Chatterjee for suggesting the problem and guiding the work during the course of investigations. The author also expresses his thanks to Miss. B.V. Rajeswari for her helpful suggestions.

Bibliography

1. W. Rotman, 'Plasma simulation by artificial dielectrics with parallel plate media' Trans. IRE., Vol. AP.10, 1962, pp. 82

2. J. Brown, 'Microwave Lenses' Methuen's Monographs on physical subjects; John Wiley and Sons, 1953.

3. Carlson and Heins; 'Reflection of an electromagnetic plane wave by an infinite set of plates' - Quarterly of Applied Mathematics, 1947, Vol.4 pp. 313.

4. Chatterjee,et.al; 'Investigations on artificial dielectrics at Microwave frequencies' - Journal of the Indian Institute of Science, Vol. 37, 1955, pp. 304.

5. Wait, 'Reflection from a wire grid parallel to a conducting plane ' Canadian Journal of Physics, 1954, Vol. 32, pp. 571-579.

6. Brown, 'Artificial dielectrics having refractive indices less than unity' Proc. IEE 1953, Vol. 100, pt. IV, pp. 51-62.

7. Macfarlane. 'Surface impedance of an infinite parallel wire grid or oblique angles of incidence Proc. IEE , Vol.93, pt. 3a,pp.1523-27

8. Ignatousky, 'Zur Theorie der Gitter' Annalen der Physik 1914, vol.44, pp.369-436

9. Ignatousky 'Hochfrequenztechnik,1939, vol.54 pp.62.

10. J.H.Richmond, 'Antenna Pattern distortion by dielectric sheets - IRE Trans on Antennas and Propagation 1956 , vol.4, pp. 139-142.

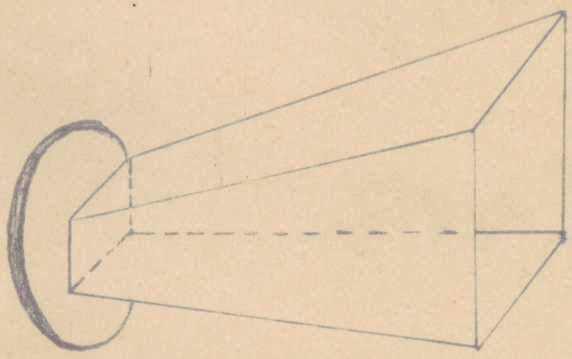

TRANSMITTING HORN.

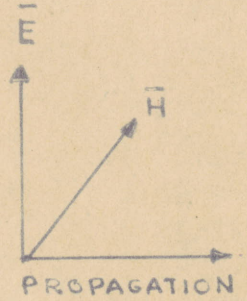

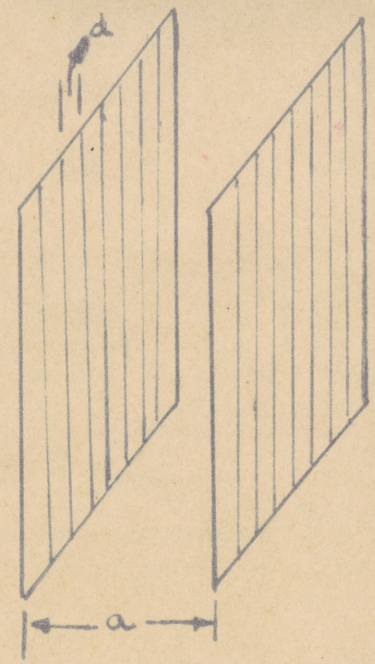

PLASMA STRUCTURES.

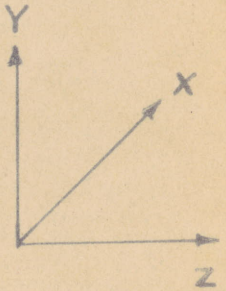

COORDINATE SYSTEM.

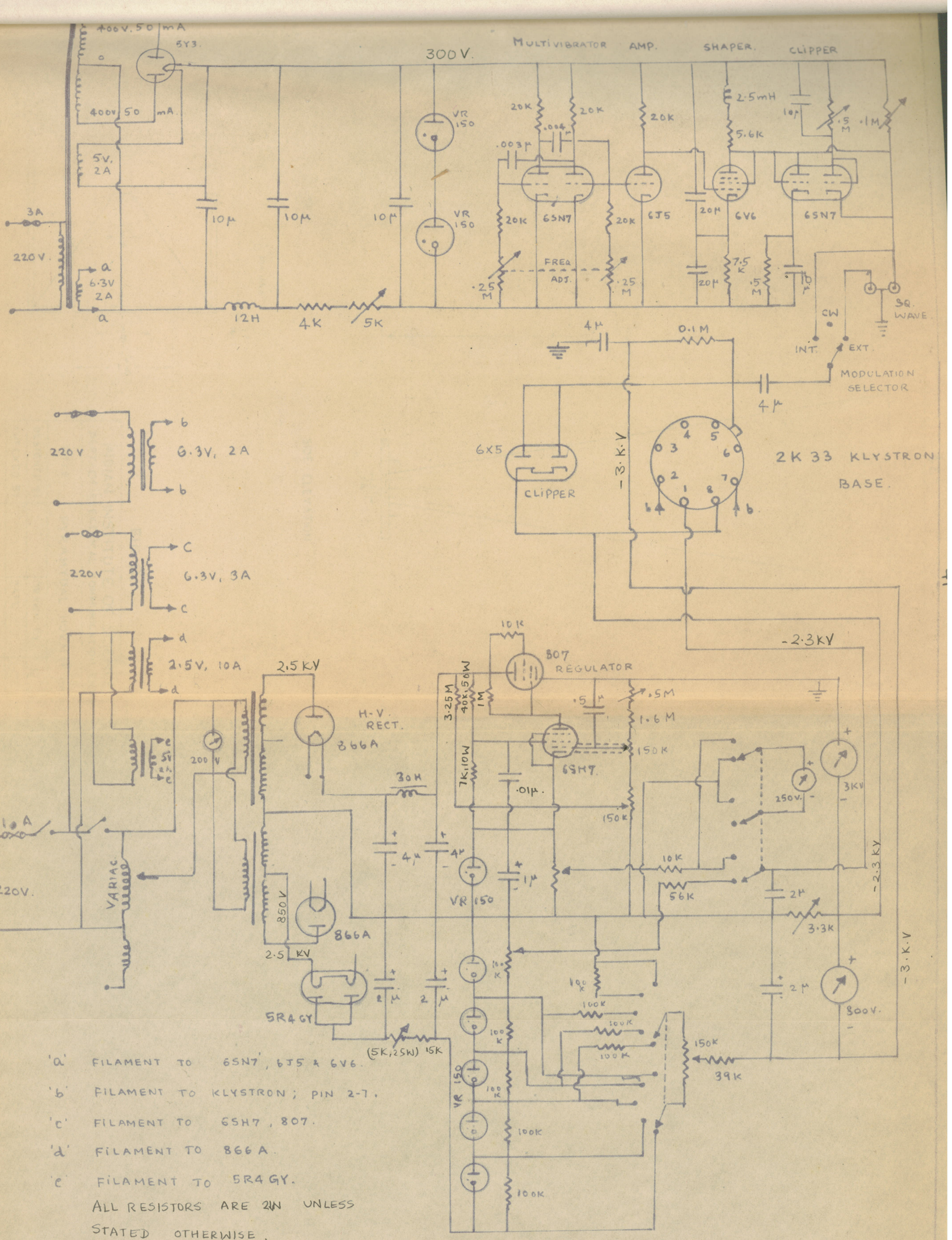

'a' FILAMENT TO 6SN7, 6J5 & 6V6.

'b' FILAMENT TO KLYSTRON; PIN 2-7.

'c' FILAMENT TO 6SH7, 807.

'd' FILAMENT TO 866A.

'e' FILAMENT TO 5R4GY.

ALL RESISTORS ARE 2W UNLESS STATED OTHERWISE.

FIG. 1, 2K-33. KLYSTRON POWER SUPPLY - CIRCUIT DIAGRAM.

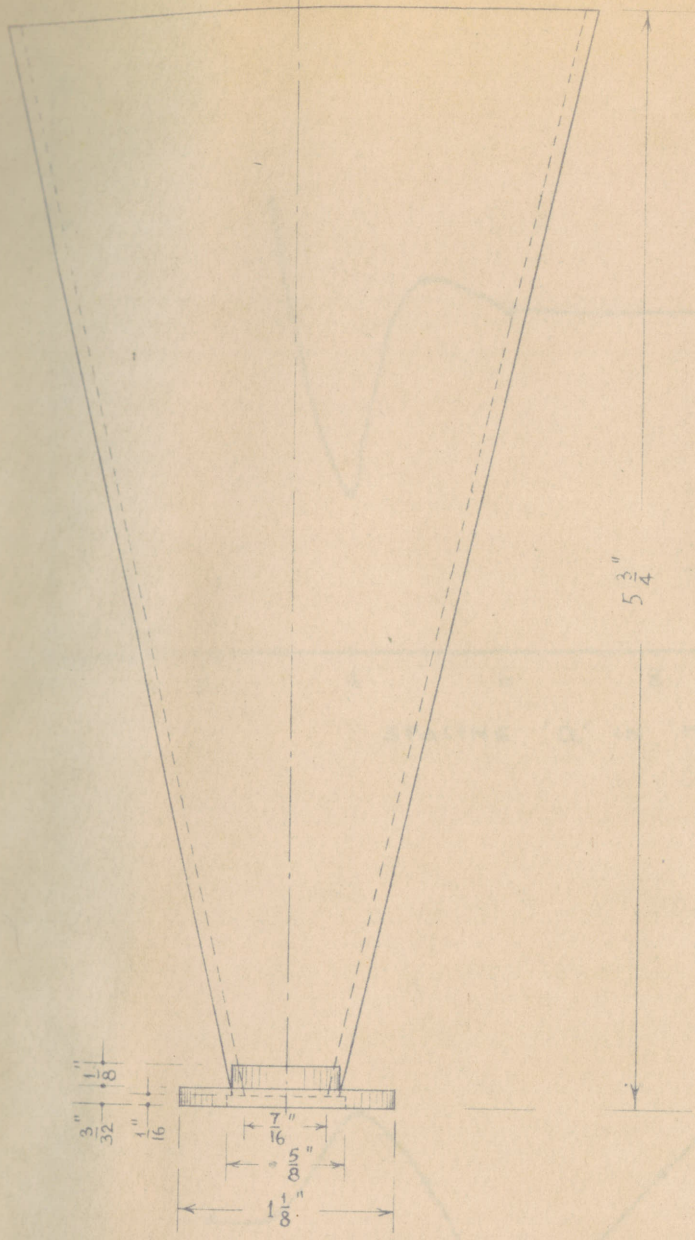

ELEVATION

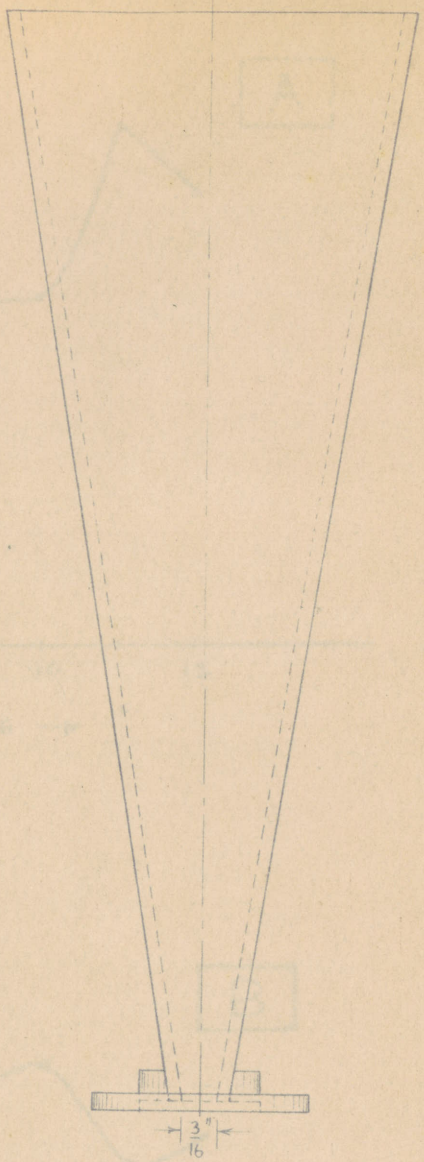

SIDE ELEVATION

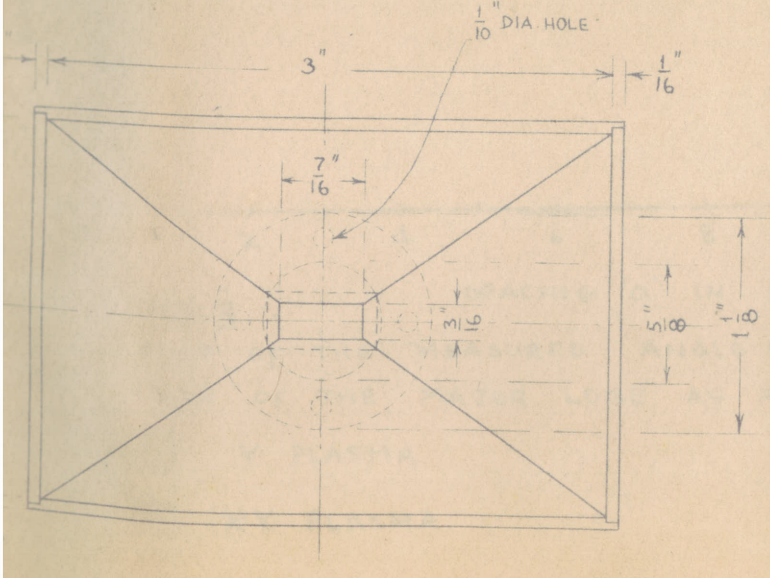

PLAN

FIG. 2.

INDIAN INSTITUTE OF SCIENCE DEPT. OF ELECTRICAL COMMUNICATION ENGG.			
TITLE	PYRAMYDAL HORN (K-BAND)		
DESIGNED BY		DRAWN BY	RW
CHECKED BY		DATE	
SCALE	FULL SIZE	DRAWING No	12-1
MATERIAL	BRASS		

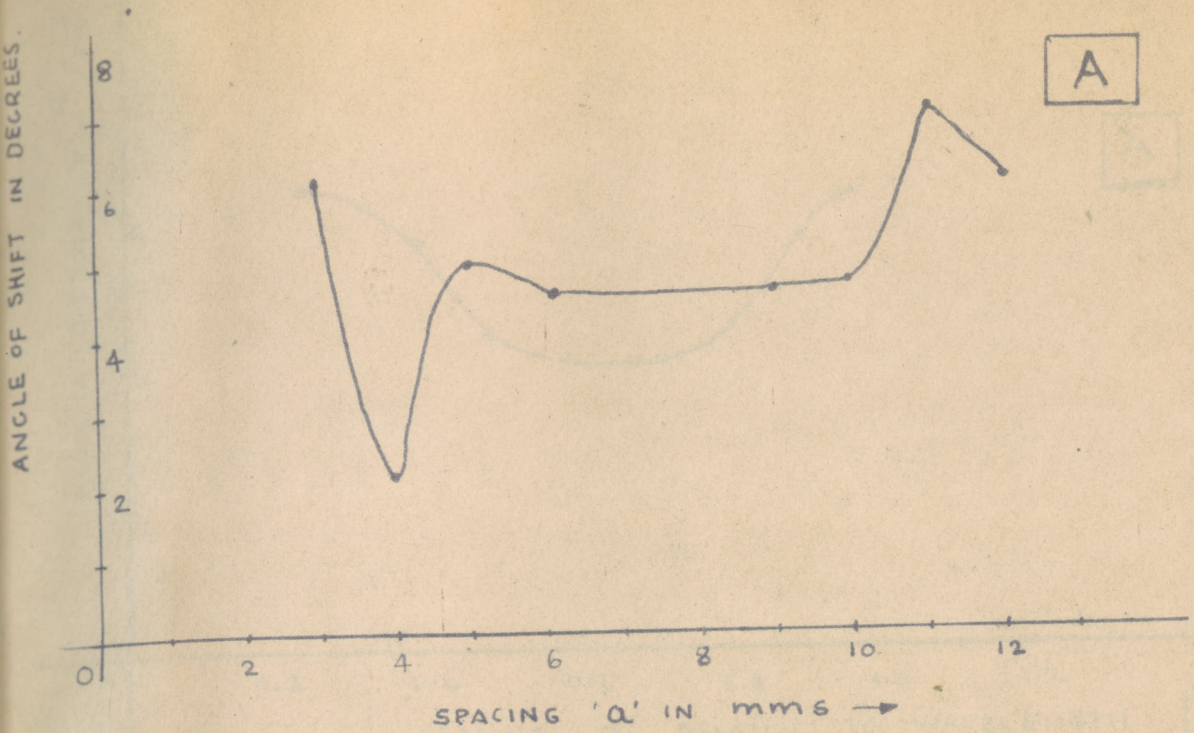

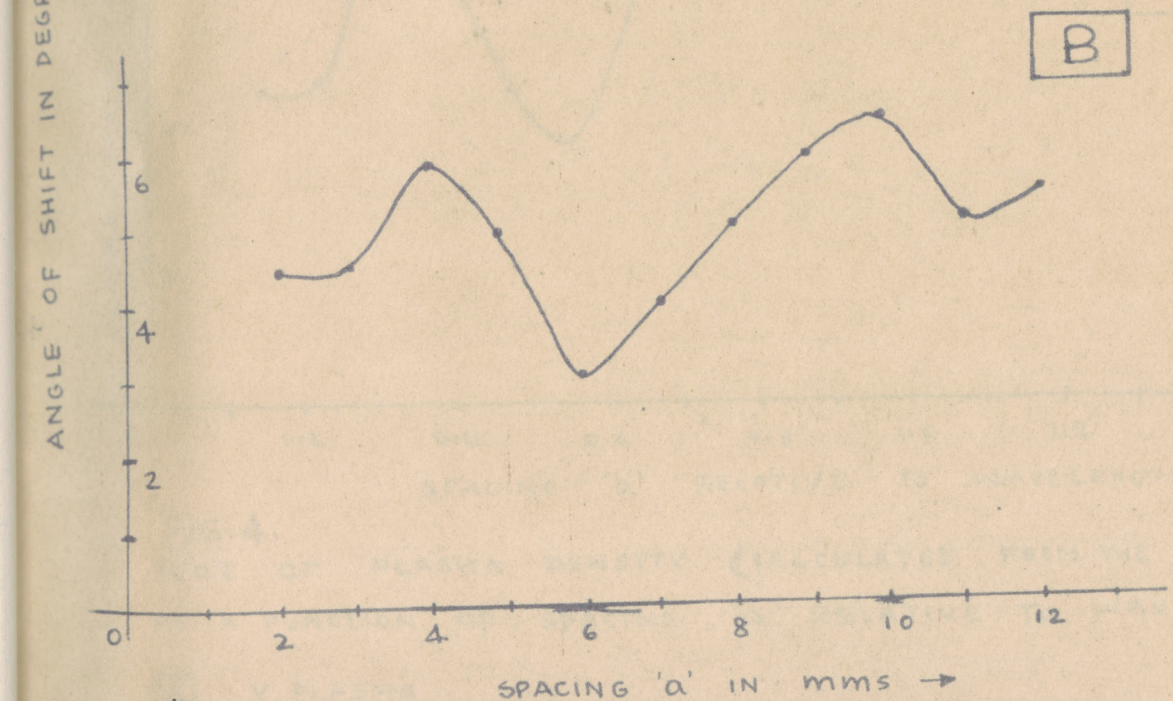

FIG.3.

PLOT OF THE MEASURED ANGLE OF SHIFT IN THE PEAK. OF THE MAJOR LOBE AS A FUNCTION OF 'a'.

[A] Y PLASMA

[B] XY PLASMA.

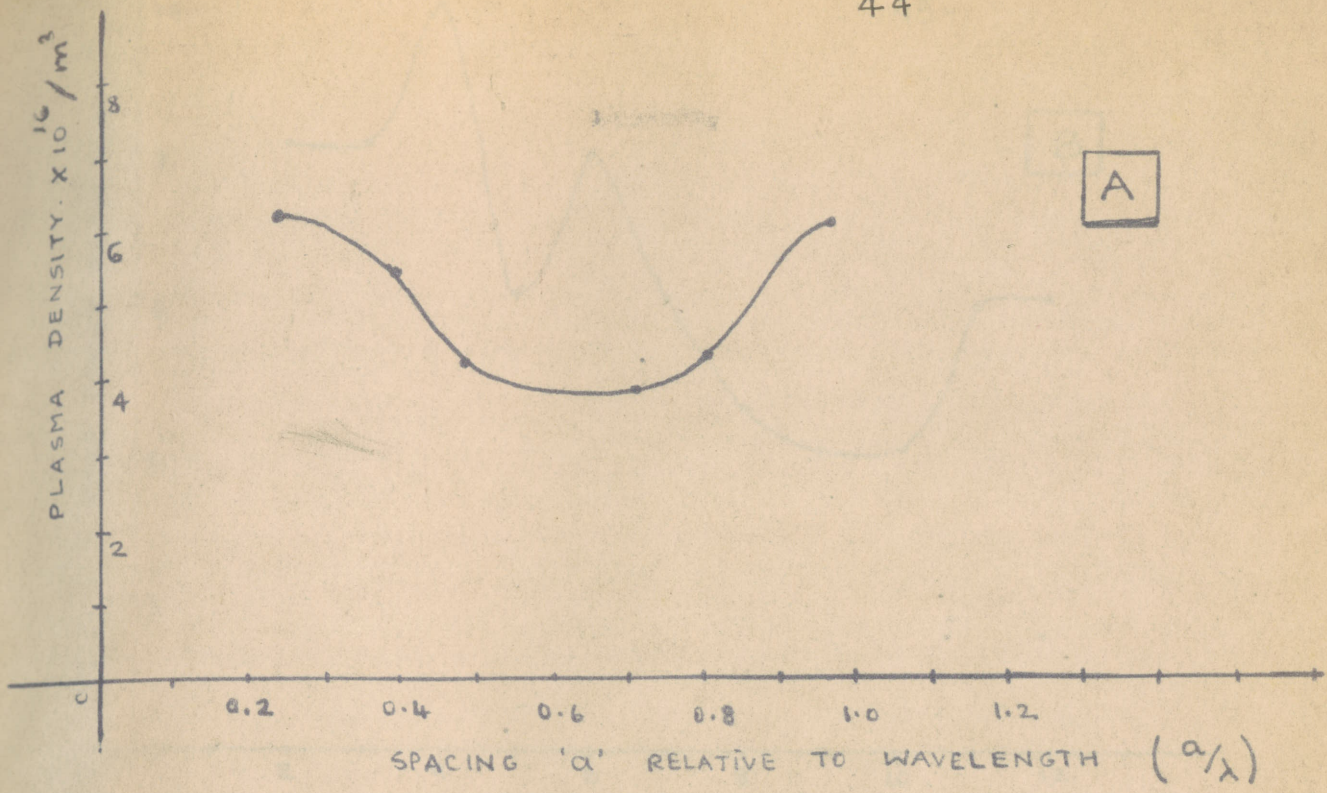

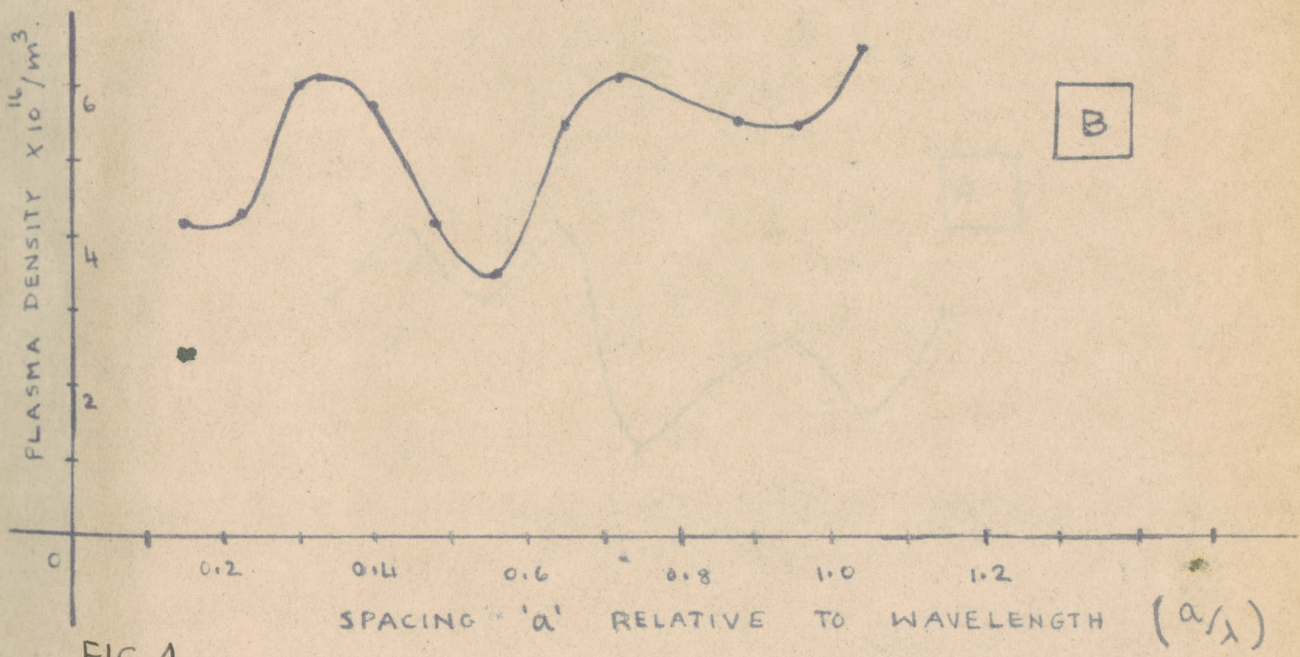

FIG. 4.

PLOT OF PLASMA DENSITY (CALCULATED FROM THE OBSERVED SHIFT) AS A FUNCTION OF SPACING 'a' RELATIVE TO WAVELENGTH (a/λ)

A Y PLASMA

B XY PLASMA.

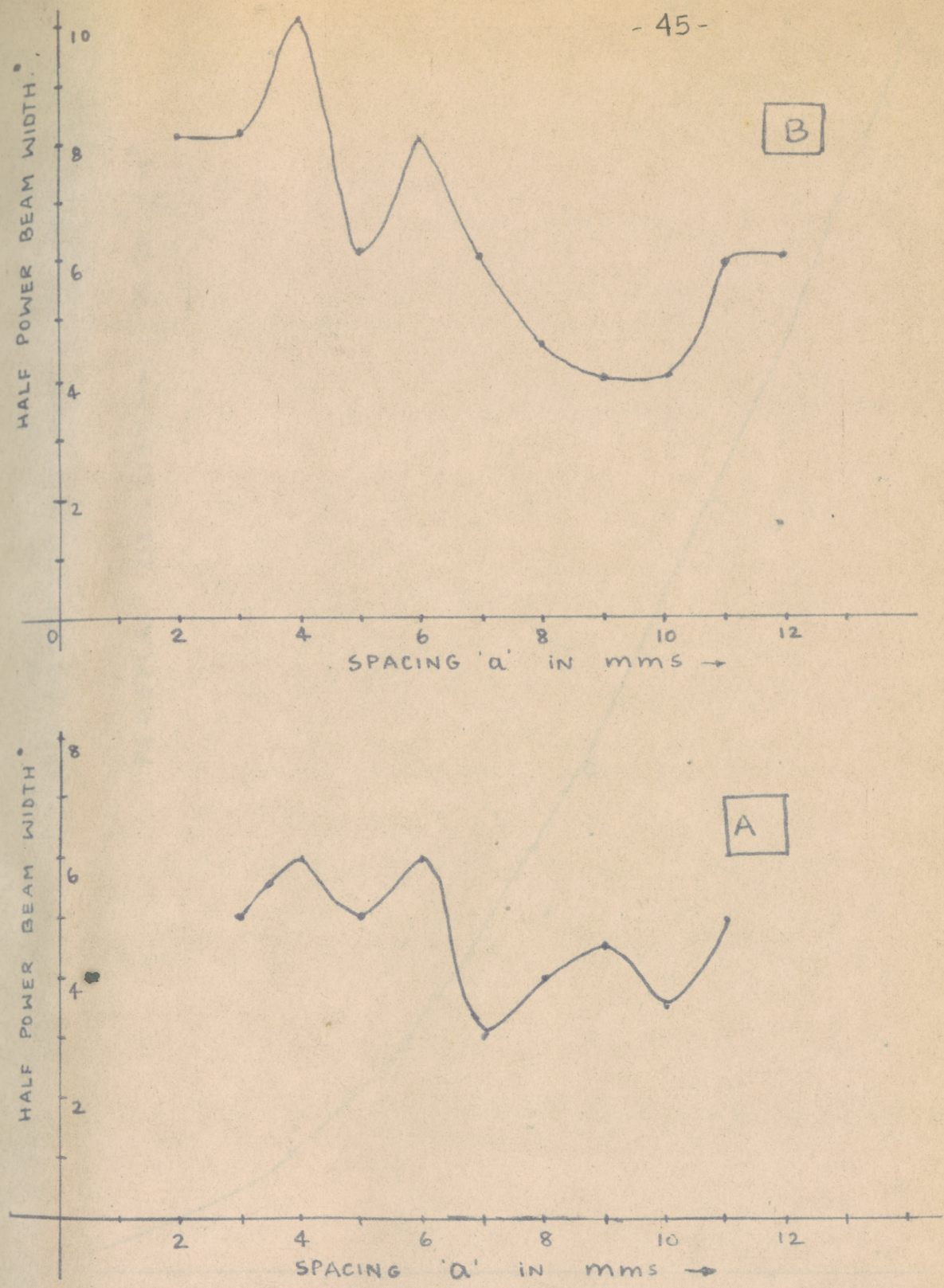

FIG. 5.

PLOT OF THE HALF POWER BEAM WIDTH OF THE MAJOR LOBE AS A FUNCTION OF SPACING 'a'.

[A] Y PLASMA.

[B] XY PLASMA.

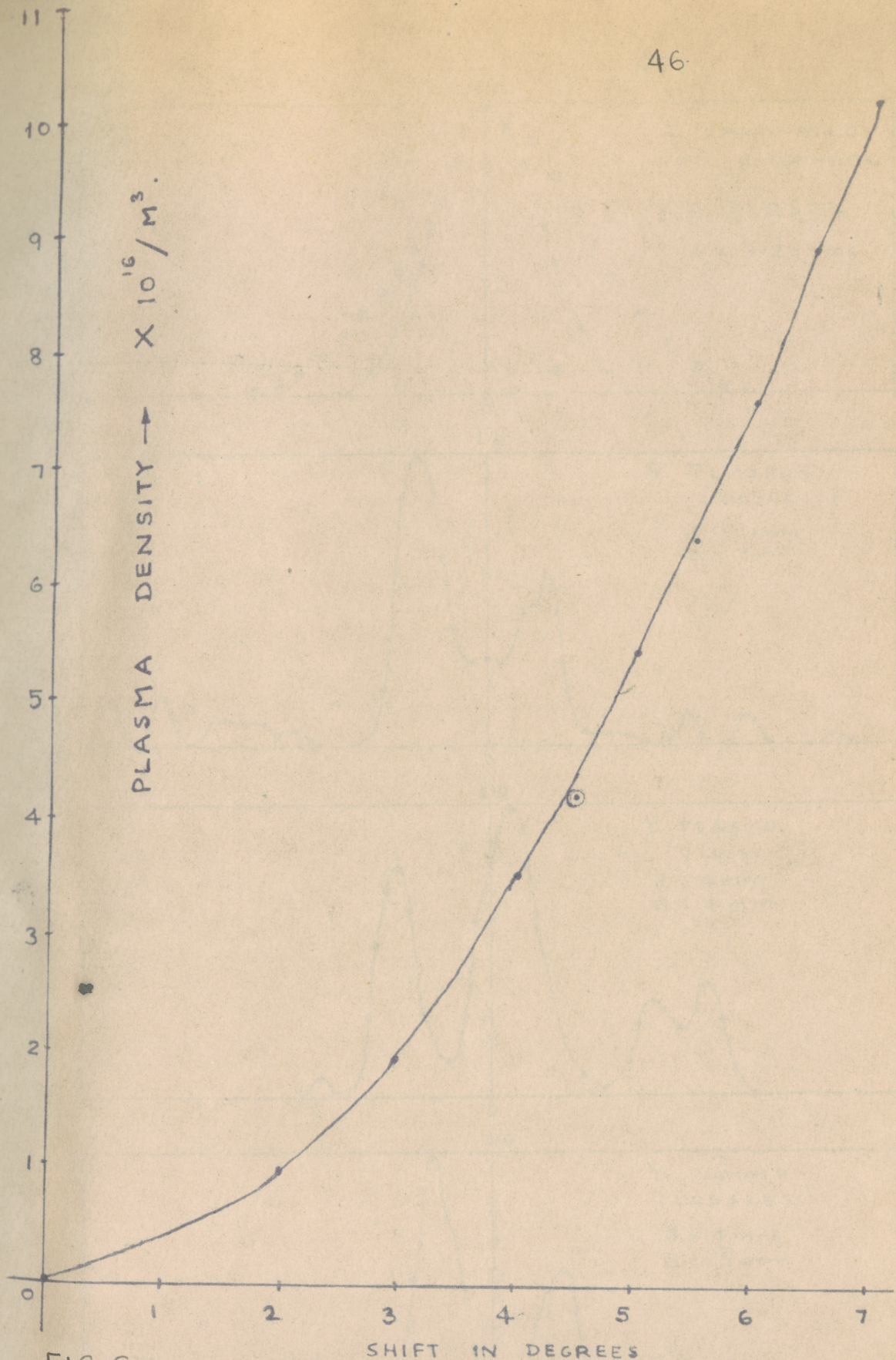

FIG.6.

PLOT OF EQUIVALENT PLASMA DENSITY AS A FUNCTION OF THE SHIFT IN THE PEAK OF THE MAJOR LOBE.

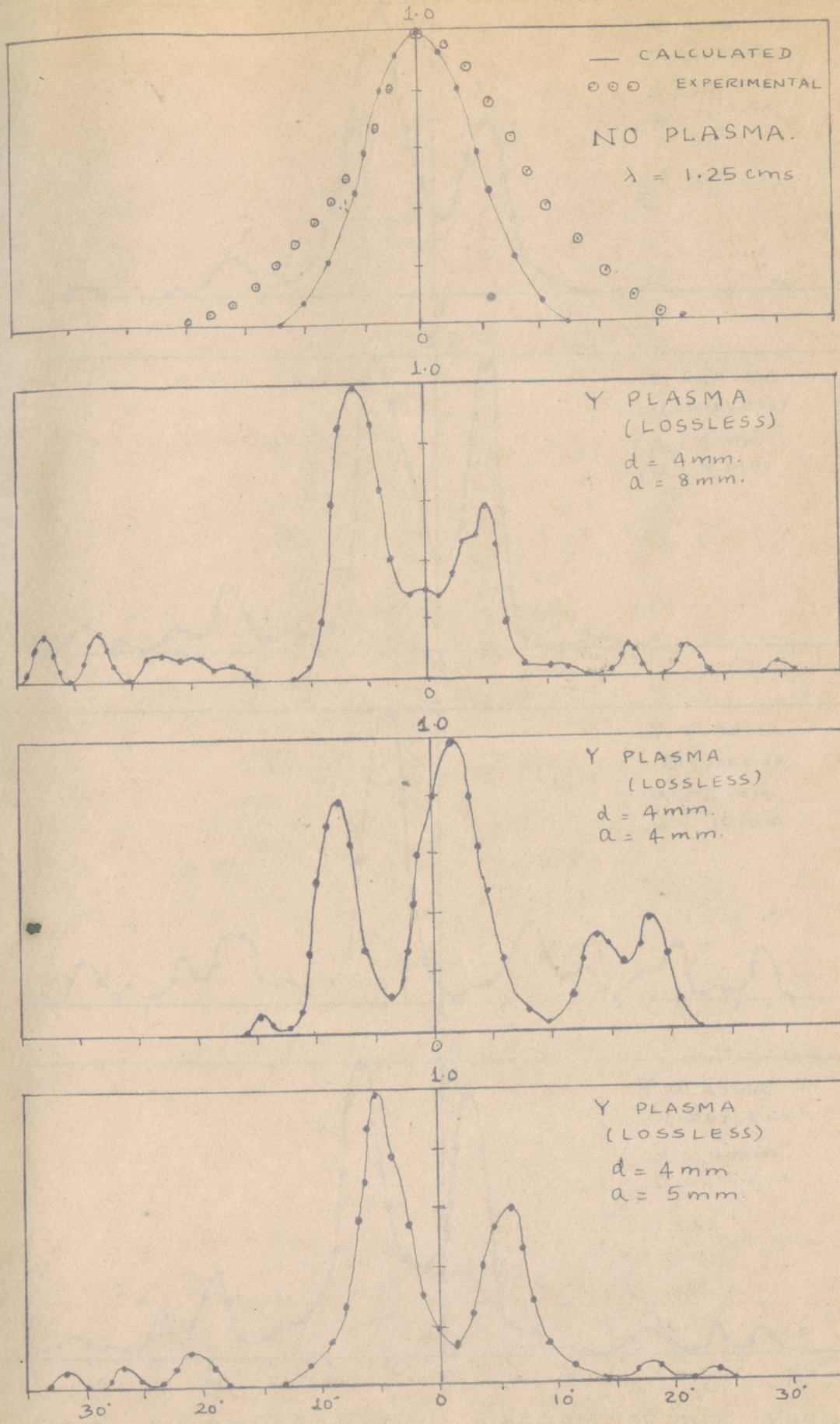

FIG. 7. H- PLANE RADIATION DIAGRAM OF THE HORN

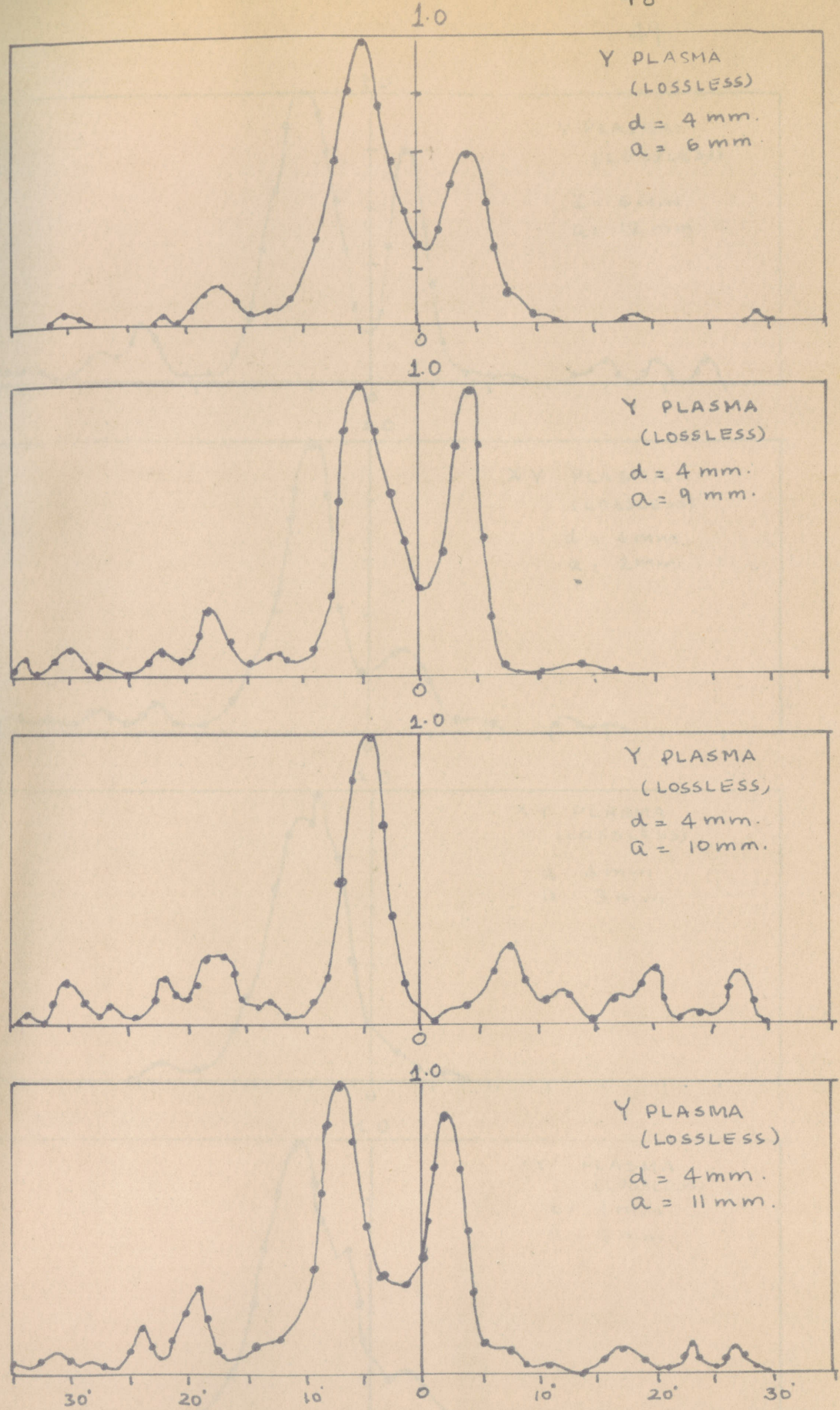

FIG. 8. H PLANE RADIATION DIAGRAM OF THE HORN IN PRESENCE OF PLASMA

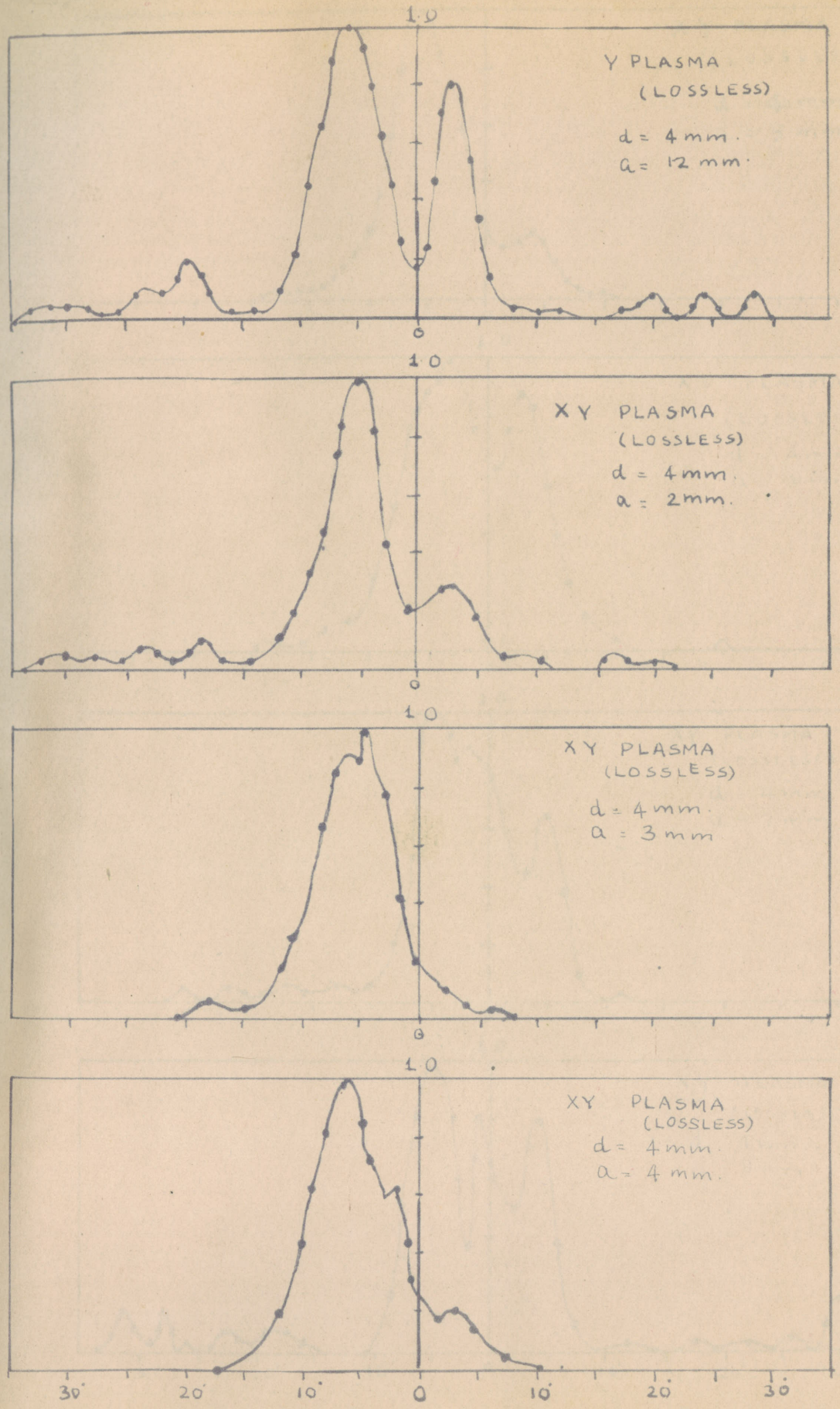

FIG 9. H PLANE RADIATION DIAGRAM OF THE HORN IN PRESENCE OF PLASMA.

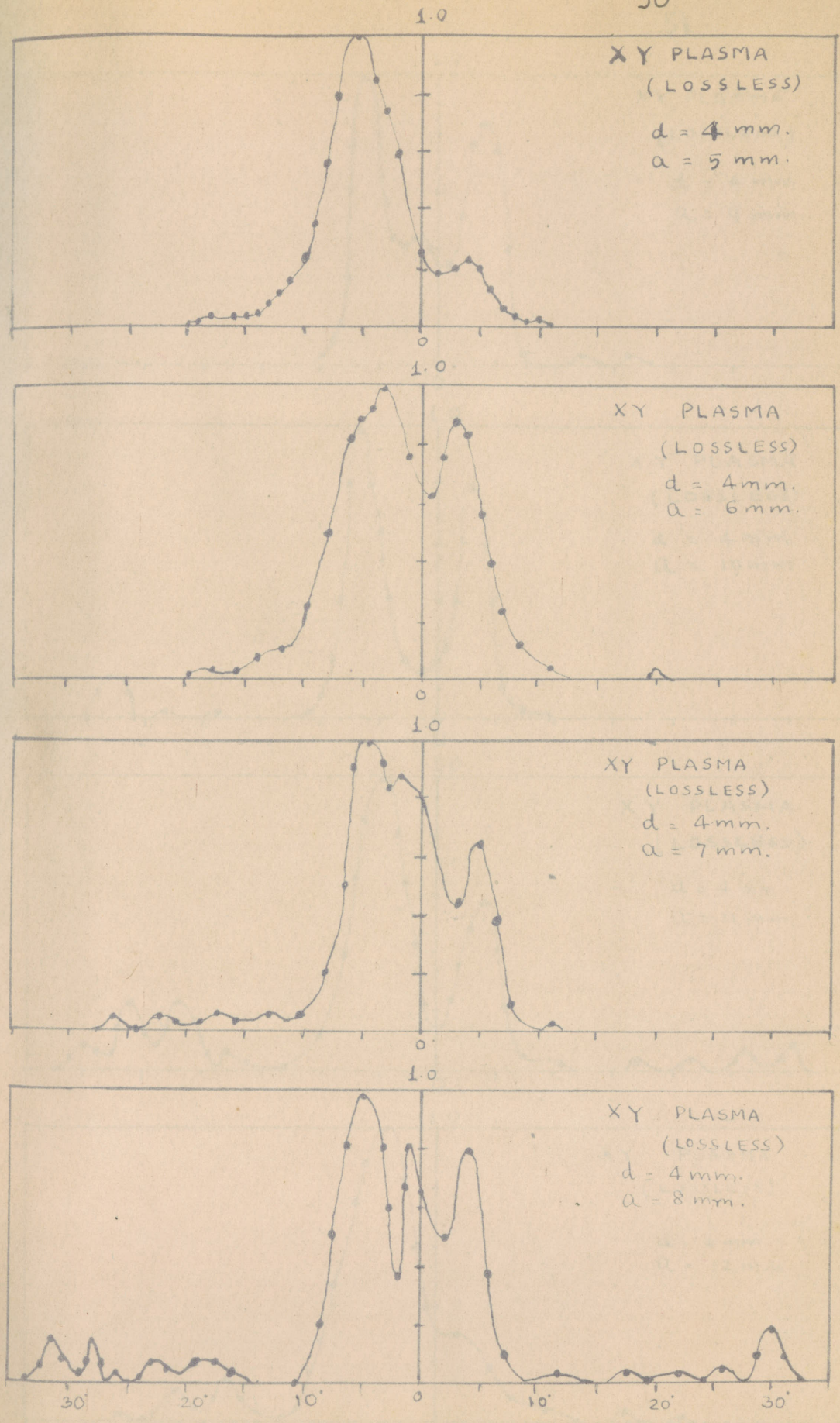

FIG 10. H PLANE RADIATION DIAGRAM OF THE HORN IN PRESENCE OF PLASMA

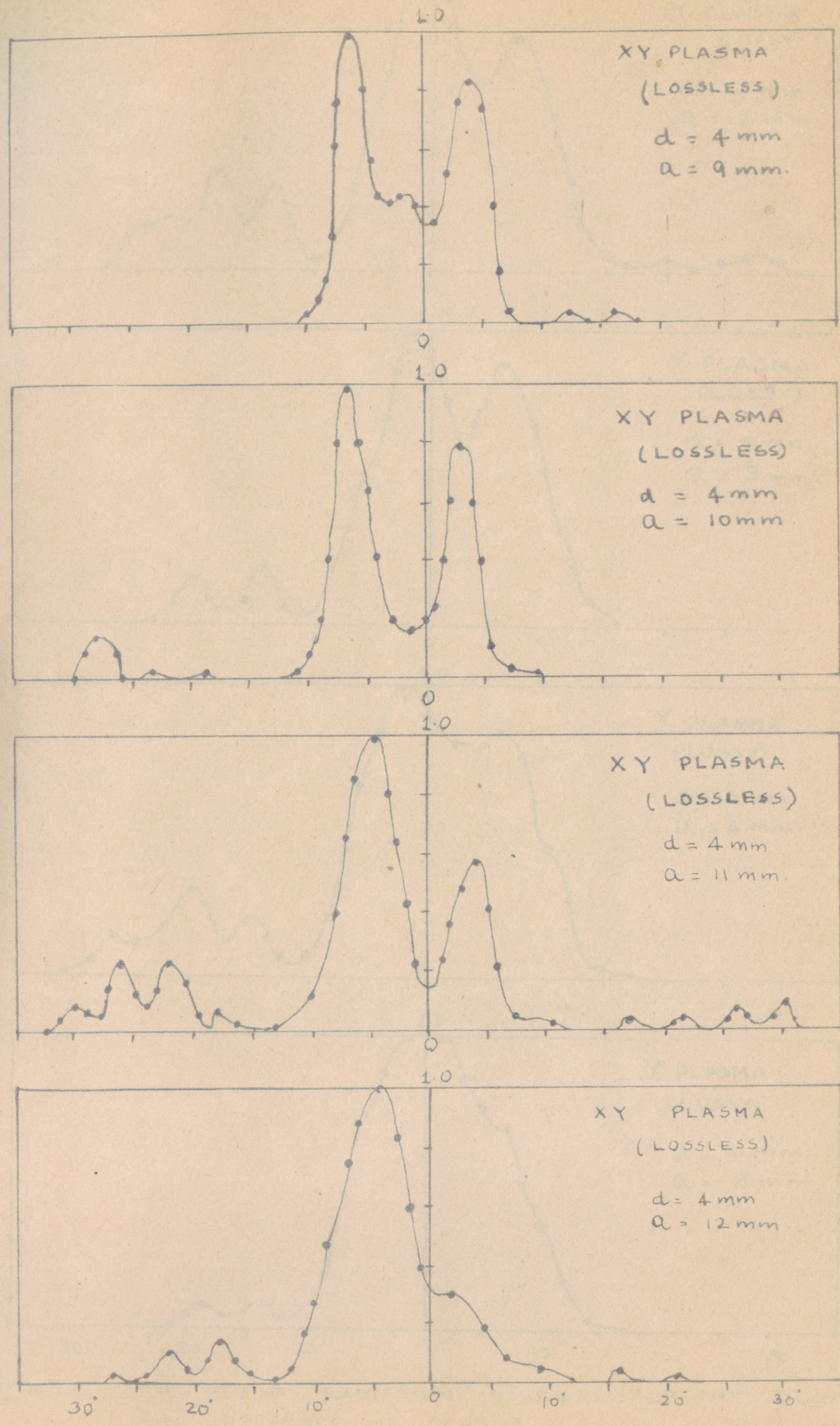

FIG. 11. H PLANE RADIATION DIAGRAM OF THE HORN IN PRESENCE OF PLASMA

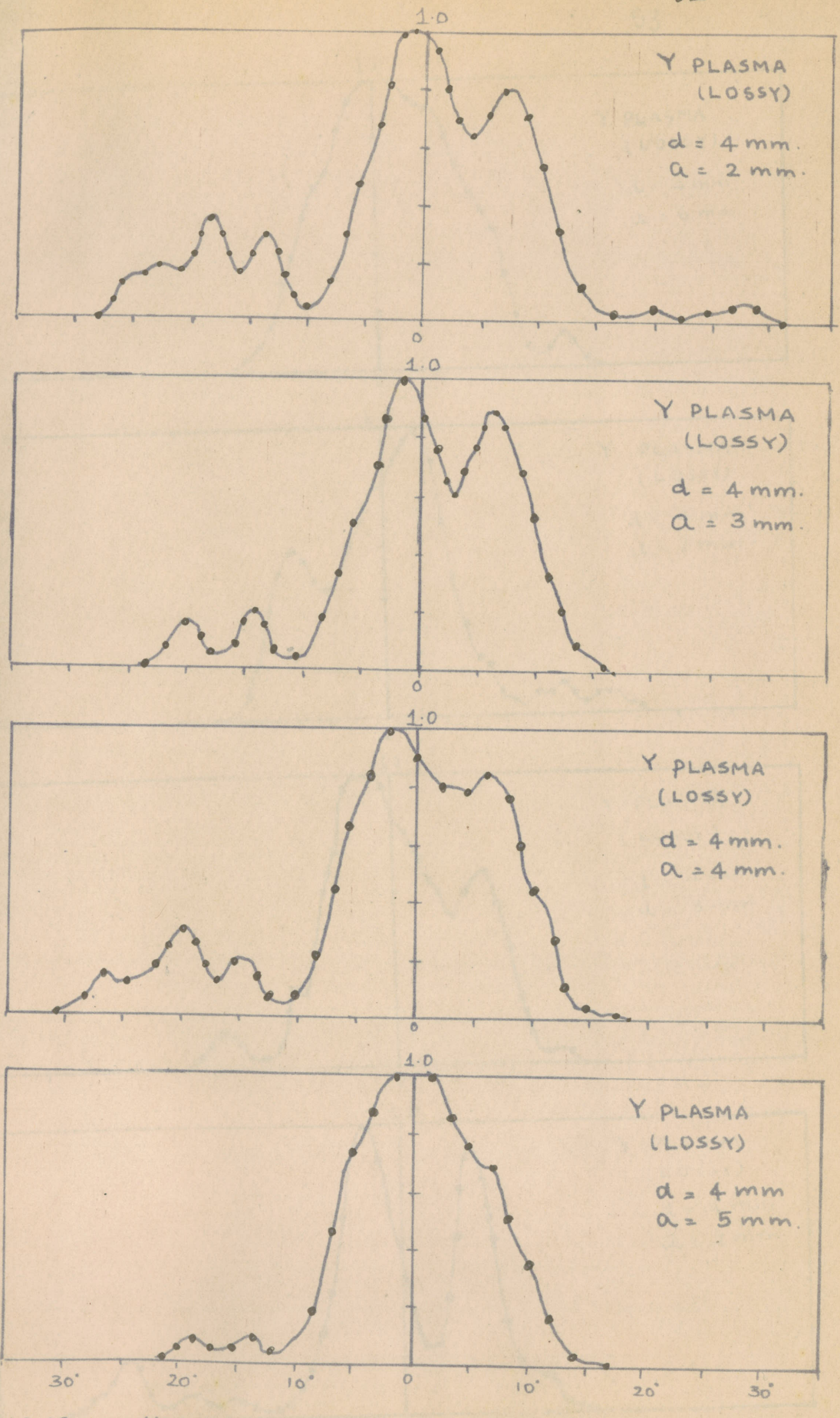

FIG.12. H- PLANE RADIATION DIAGRAM OF THE HORN IN PRESENCE OF PLASMA.

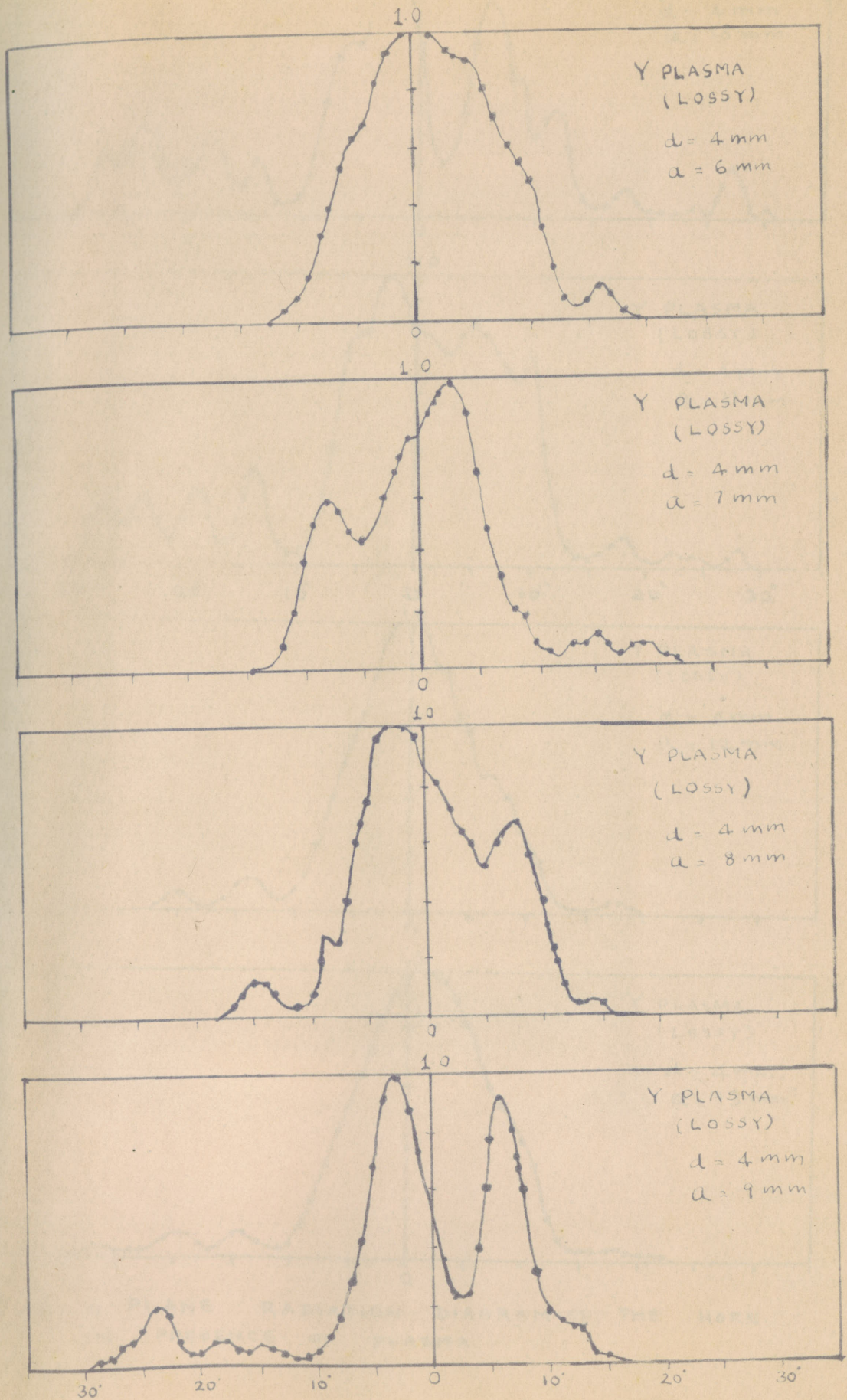

FIG. 13. H PLANE RADIATION DIAGRAM OF THE HORN IN PRESENCE OF PLASMA.

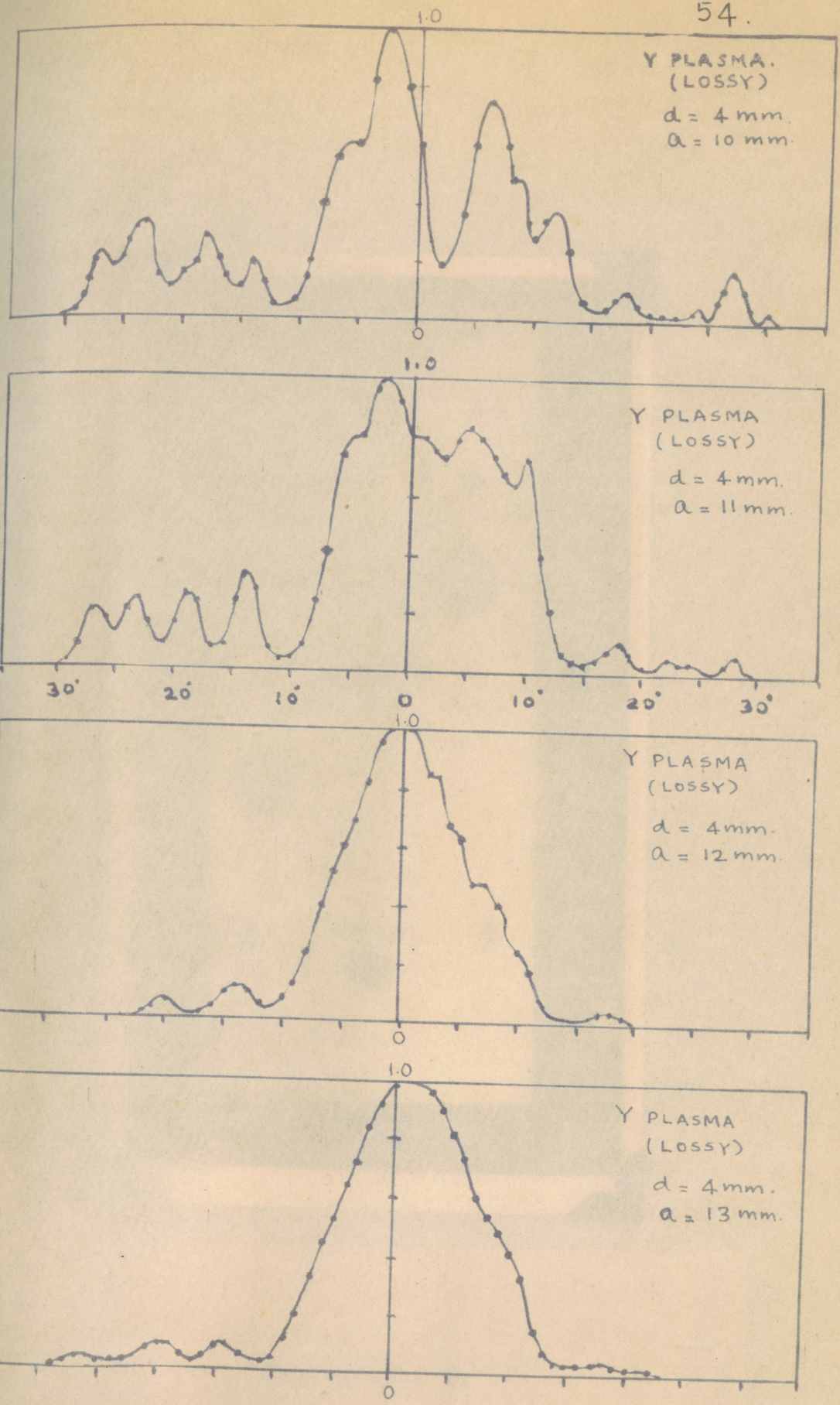

FIG. 14. H PLANE RADIATION DIAGRAM OF THE HORN. IN PRESENCE OF PLASMA.

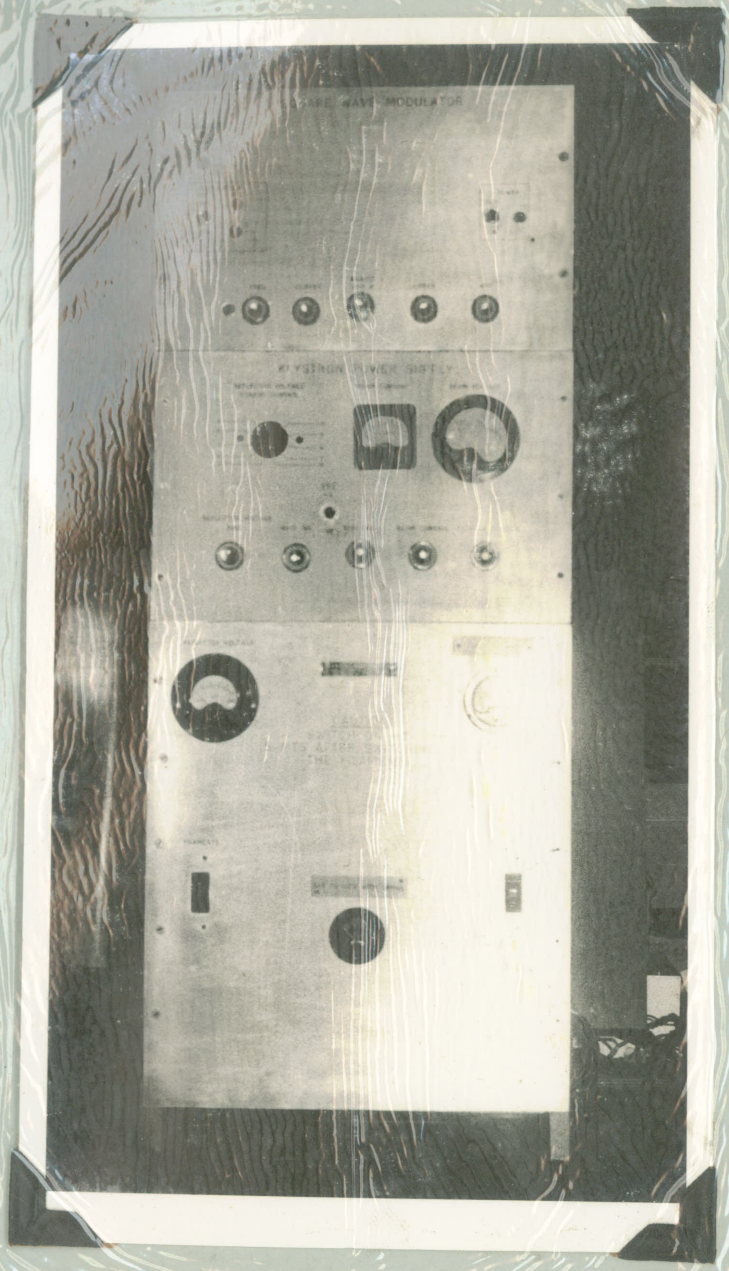

Photograph. 1.

2K-33 Klystron Power Supply Unit
with a Square wave Modulator.

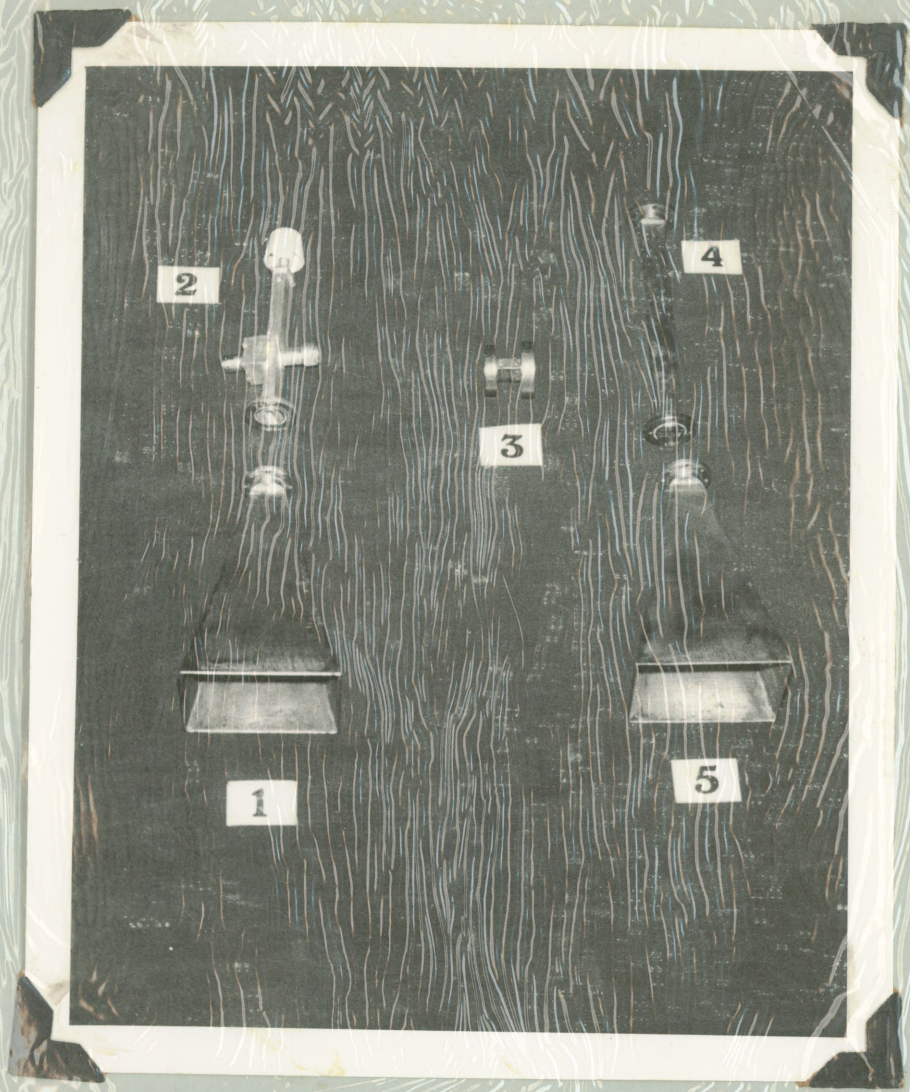

Photograph. 2.

K Band Microwave Components Fabricated.

1. Pyramidal Horn.(Transmitter)
2. Detecting Section.
3. Waveguide Adapter.
4. 6″ Waveguide section.
5. Pyramidal Horn.(Receiver)

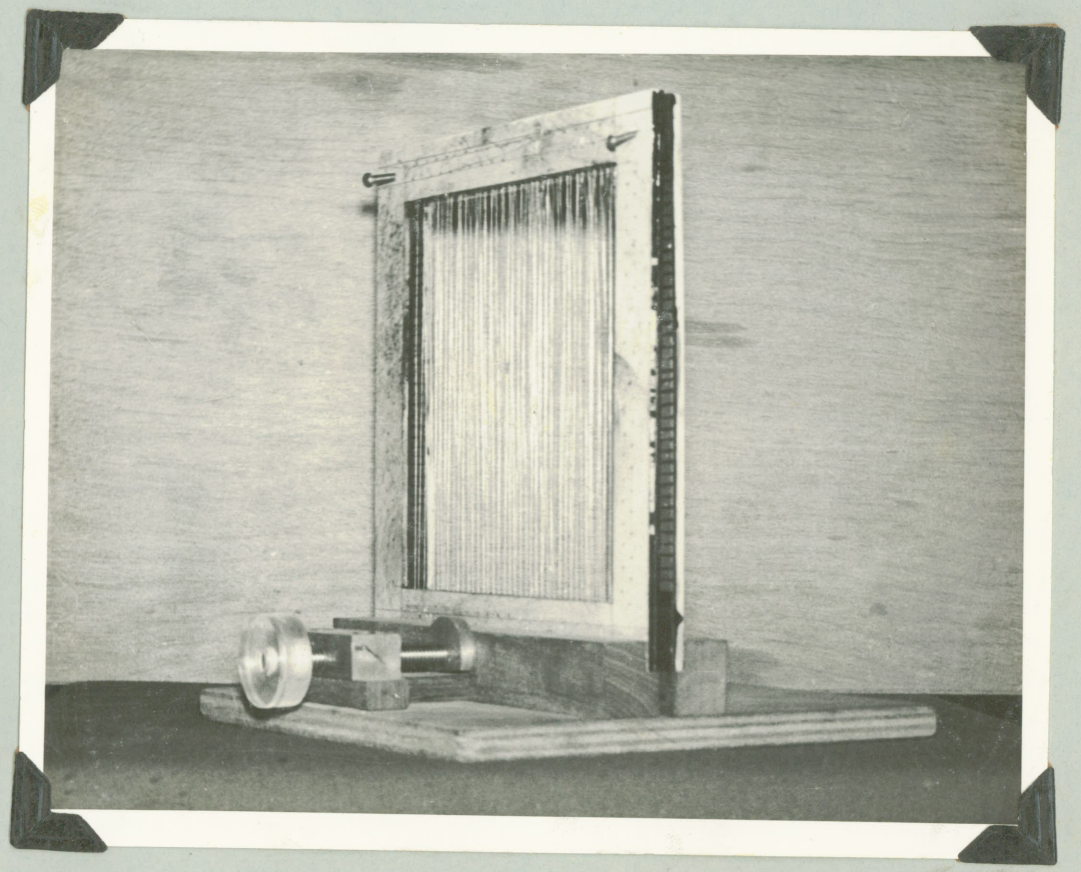

Photograph. 3

Slow Motion Drive facility to vary the distance of Separation between two structures.

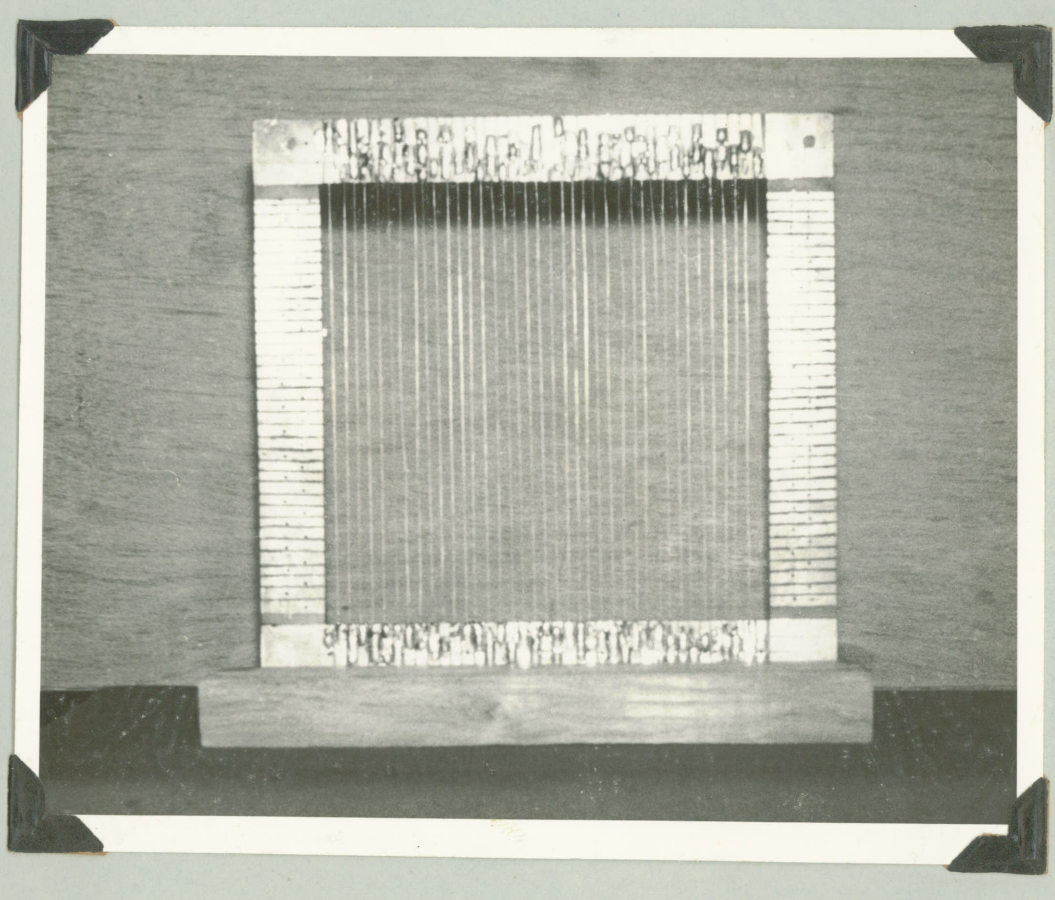

Photograph. 4

Lossless Y Plasma Structure.

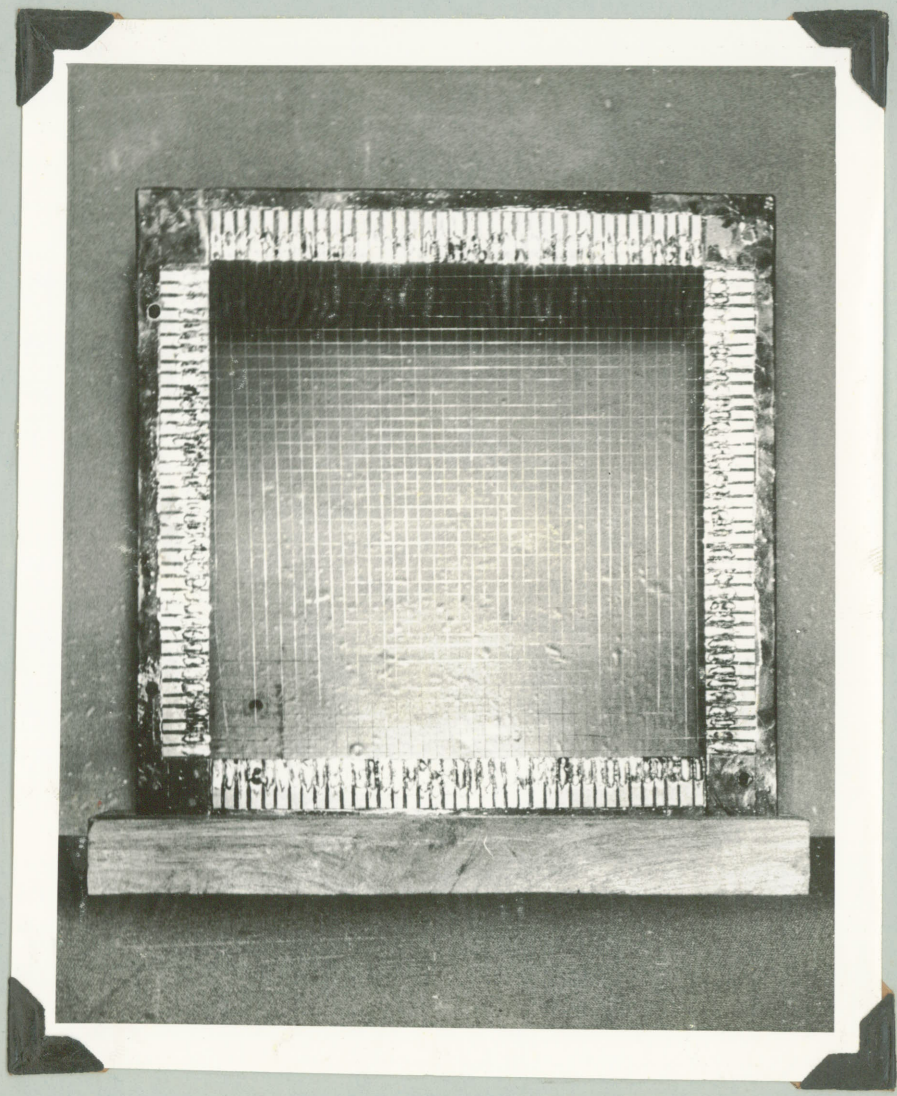

Photograph. 5

Lossless XY Plasma Structure.

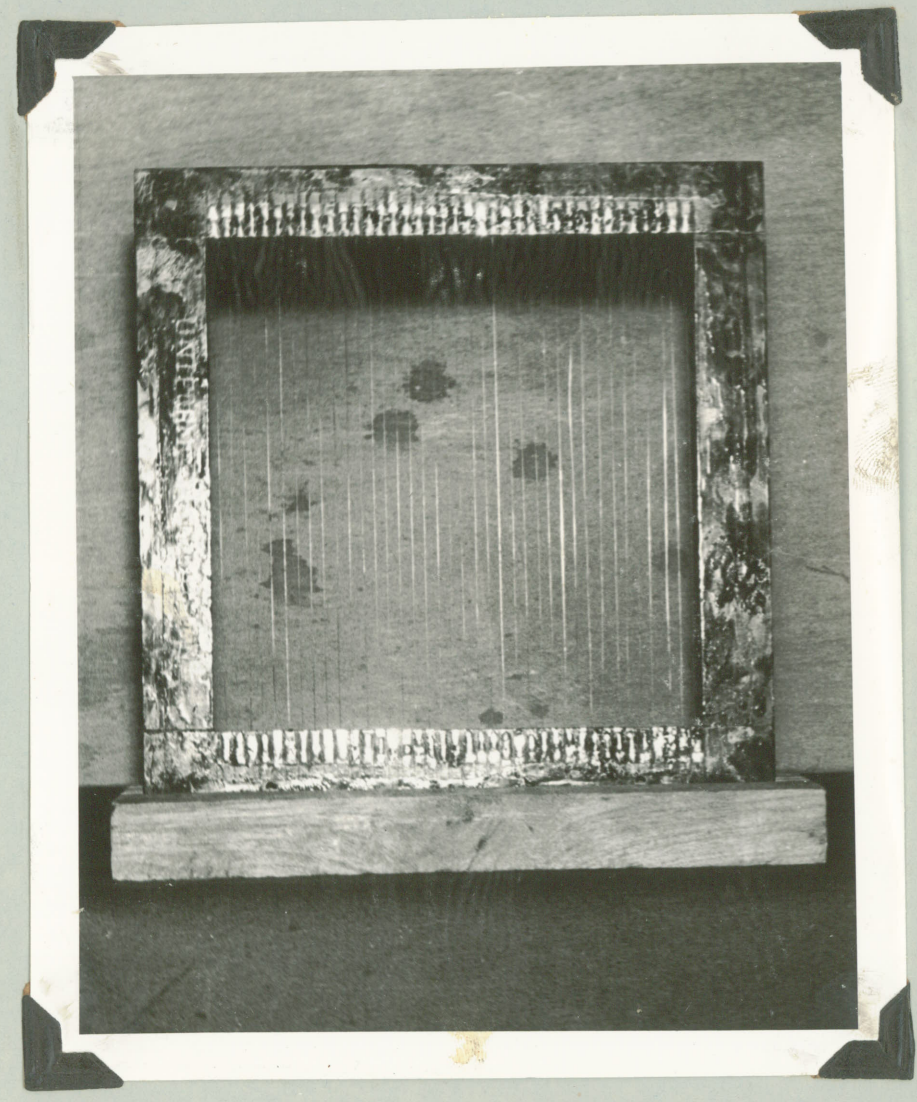

Photograph. 6

Lossy Y Plasma Structure.

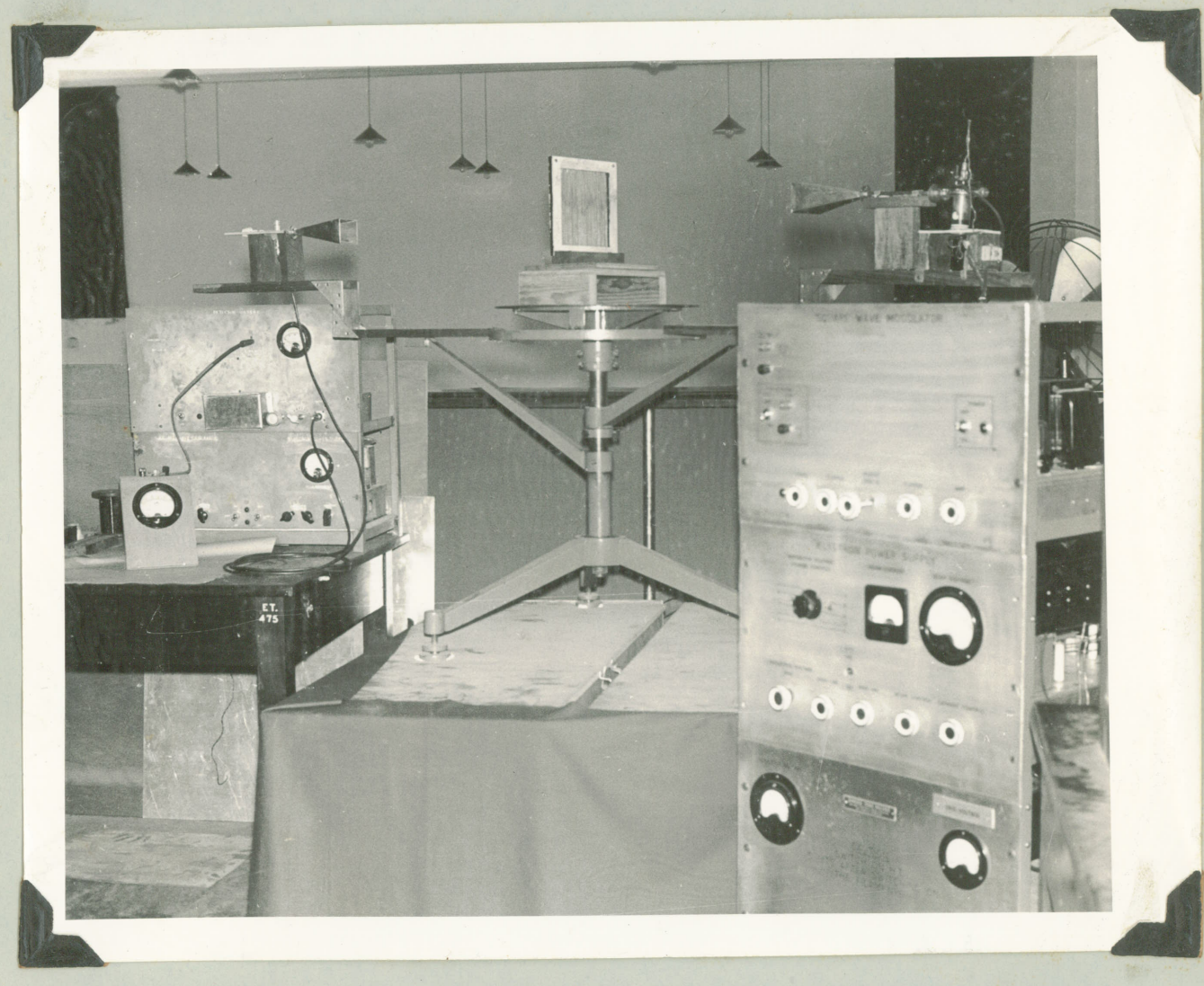

Photograph. 7

Experimental set-up.